FINAL PUBLISHABLE JRP REPORT

JRP-Contract number	**ENG57**
JRP short name	**VITCEA**
JRP full title	**Validated inspection techniques for composites in energy applications**
Version numbers of latest contracted Annex Ia and Annex Ib against which the assessment will be made	Annex Ia: V1.0 Annex Ib: V1.0
Period covered (dates)	From 1st July 2014 To 30th June 2017

JRP-Coordinator

Name, title, organisation	Mr Michael Gower, Principal Research Scientist, National Physical Laboratory
Tel:	+44 20 8943 8625
Email:	michael.gower@npl.co.uk

JRP website address: http://projects.npl.co.uk/vitcea/

JRP start date and duration:	1st July 2014, 36 months
JRP-Coordinator: Michael Gower, Mr, NPL Tel: +44 20 8943 8625 E-mail: michael.gower@npl.co.uk JRP website address: http://projects.npl.co.uk/vitcea/	
JRP-Partners: JRP-Partner 1: NPL, United Kingdom JRP-Partner 2: BAM, Germany	 JRP-Partner 3: CMI, Czech Republic JRP-Partner 4: PTB, Germany
REG1-Researcher (associated Home Organisation):	Steve Mahaut CEA, France

EMRP European Metrology Research Programme
Programme of EURAMET
The EMRP is jointly funded by the EMRP participating countries within EURAMET and the European Union

TABLE OF CONTENTS

1 Executive Summary 3
2. Project context, rationale and objectives 4
3. Research results 6
4. Actual and potential impact 30
5. Website address and contact details 33
6. List of publications 33

1 Executive Summary

Introduction

This project has made a significant contribution to the establishment of a validated measurement infrastructure for the detection of manufacturing defects and in-service damage in a range of fibre-reinforced polymer (FRP) composites used in various energy sector applications. We have developed validated operational procedures for five non-destructive evaluation (NDE) techniques that will form the pre-cursors of NDE-FRP composite specific standards; the first of their kind outside of the aerospace industry. Through future standardisation of these procedures, our research will result in EU organisations achieving significant reductions in operation and maintenance costs associated with energy generating plant, as well as greenhouse gas emissions through reduced fossil fuel consumption of lighter weight vehicles facilitated by the increased use of FRP composites.

The Problem

The excellent mechanical properties of fibre reinforced plastic (FRP) composites gives them considerable advantages for use in renewable energy (wind, wave and tidal), oil and gas, and transport applications, thus enabling the EU to achieve reductions in fossil fuel reliance, energy consumption and greenhouse gas emissions. However, FRP composites can contain a diverse range of defects and damage mechanisms that can reduce the strength, stiffness and life of a structure. These can be difficult to detect, but reliable non-destructive evaluation (NDE) would aid characterisation of FRP material quality and encourage their full exploitation. Despite many innovations in the development of NDE for the assessment of defects and damage, relatively few methods are commonly used. This is mainly because standardised operational procedures are not available, and there are perceptions that NDE is too unproven, costly or complex. There are currently no International Organization for Standardization (ISO) standards for NDE in existence that are specific to defect detection in FRP composites. Several American Society for Testing Materials (ASTM) composite specific NDE standards are available, but these tend to be focused on the aerospace sector and do not provide enough detail and validated data on issues such as probability of detection (POD), defect size and location sensitivity. Therefore improved NDE operational procedures and standards are required to enable the increased use of FRPs for energy applications are needed.

The Solution

The solution involved developing validated operational procedures for microwave, active thermography, laser shearography, phased array ultrasonics and air-coupled ultrasonics NDE techniques. The applicability and suitability of the techniques for defect detection in FRP products post fabrication and their subsequent in-service assessments, was evaluated using a range of reference defect artefacts (RDAs) and natural defect artefacts (NDAs) that were designed and manufactured from a range of FRP composites typically used in energy applications. RDAs were manufactured to have artificially created defects, with well-defined dimensions and in known positions, and NDAs were fabricated by overloading to introduce damage that was more representative of that which actually occurs in service. These operational procedures were then validated via intercomparison and probability of detection (POD) assessments. In addition, new modelling capability for each NDE technique (with the exception of laser shearography) was developed in order to assess whether simulations of inspection scenarios could be used to supplement data obtained via POD assessments with the aim of reducing the associated cost and time requirements. Extensive characterisation of the materials used in the RDAs and NDAs was undertaken to provide the material property input data for these models.

Impact

The project developed a total of thirteen sector specific RDAs, NDAs and POD-RDAs, as well as operational procedures for ultrasonic (phased array, air-coupled), microwave, active thermography, and laser shearography NDE techniques. These are freely available via NMI project partners. Additional measurement services of the thermal properties of composite materials are now available from NPL and CMI, and improved optical property measurement services have been developed by PTB; emissivity of anisotropic composites under vacuum can now be measured with an uncertainty of 0.005. New modelling capabilities were developed at BAM, PTB and REG(CEA) for ultrasonic phased array, microwave and active thermography NDE techniques, enabling theoretical POD assessments to be undertaken. A UK based engineering consultancy company has used the microwave inspection facility evaluated by NPL to inspect

glass fibre-reinforced plastic (GFRP)-balsa and GFRP-balsa-metal reference samples. The company were impressed by the facility and wish to evaluate it further on additional samples. As a result of the project, a manufacturer of microwave inspection equipment is planning potential modifications to its microwave transducers to eliminate/reduce unwanted standing wave formations. The company has acquired the same modelling software that was used in the project for simulation of microwave inspection as a tool to improve their equipment design. The modelling work undertaken by REG(CEA) has extended the capability of the CIVA ultrasonic software, and therefore enhanced their services.

The outputs of the project will benefit end-users, designers and NDE communities involved with the use of FRPs in energy applications. They will also enable integration of novel NDE techniques, allowing improved design, manufacturing and assembly of FRPs with NDE inspection being facilitated throughout the life-cycle of FRPs.

2. Project context, rationale and objectives

Need: The use of FRP composites provides a number of advantages including lighter weight, better mechanical and environmental performance and reduced costs compared to more traditional materials. The potential benefits of increasing FRP composite usage in different industry sectors are highlighted within the UK Composites Strategy (produced by the UK Department for Business, Innovation and Skills (BIS), 2009). Most notably, the biggest opportunity for growth is identified as the wind energy sector with FRPs enabling larger, stronger and more durable turbine blades to be built. The wave and tidal sector is also seen as a key growth area as composites will enable the design of innovative, durable and corrosion resistant devices for generation of power from river and coastal resources. In the oil and gas sector, the strategy highlights the benefits of utilising composites to rehabilitate corroded steel structures and develop solutions to discover and access untapped energy reserves off shore and at greater depths. Finally, the benefit of lightweight composites in transport (aerospace, automotive, rail and marine) applications is highlighted as a key enabler to reducing fossil fuel consumption and greenhouse gas emissions, and increasing transport efficiencies.

However, widespread further adoption of FRP composites is hindered by the large number and diverse nature of defect types and complex multiple failure mechanisms compared to metals. Thus, there is a requirement for a range of validated NDE techniques with contrasting detection capabilities for the identification and sizing of defects that directly impact component performance and working life. These requirements are in direct alignment with the recommendations of the UK Materials Knowledge Transfer Network (KTN) document “A Landscape for the Future of NDT in the UK Economy”, which states:

- Mid Technology Readiness Level (TRL) technology development, validation and technology transfer for emerging NDE techniques,
- The development of recognised standards for emerging NDE technologies,
- Improving the quantification of inspection performance and reliability,
- Demonstrator schemes to incentivise uptake of new NDE technology and of existing technology in new applications.

From a regulatory perspective, there are several high level EU Directives and policies relating to emissions reduction and renewable energy targets, which are highly pertinent to, and drive the increased application of composites for lightweight applications. These are:

- Directive 2009/28/EC implementation and enforcement of the Renewable Energy Directive, which includes a 20 % renewable energy, target by 2020 for the EU. This target has also been adopted by the UK Government with the biggest contributor being wind energy,
- Directive 2009/29/EC revised EU Emissions Trading System (ETS),
- EU energy policy for 2050 (European Wind Energy Association (EWEA), March 2011) targeting an 80 % - 95 % reduction in greenhouse gas emissions.

Composite materials will play a key role in achieving the objectives and targets of these Directives and policies, and hence their acceptance for new and safe applications must be underpinned by the availability of reliable NDE techniques, procedures and data. An increase in the use of FRP composite materials for a

particular energy application, for example wind turbines, will enable the asset owner to reduce greenhouse gas emissions via lower energy production and construction processes, and reduced transportation loading. This will enable them to sell (or trade) their now excess emissions permits to organisations who wish to increase their emissions limit. Increased acceptance of FRPs will foster new and improved energy applications such as the introduction of larger more efficient turbine blades, light weighting of vehicles to reduce fuel consumption and rehabilitation of ageing steel oil and gas infrastructure, as well as offering new solutions to accessing remote oil and gas supplies. However, current standards for composite repairs on pipes and vessels used in the oil and gas industry, such as ISO/TS 24817, provide little guidance on which inspection techniques and procedures should be used, but instead refer the operator back to the repair system supplier.

The EWEA Strategic Research Agenda (EWEA SRA) identified a number of showstoppers, barriers and bottlenecks to wind energy development. The EWEA SRA identified the following issues that highlighted the need for the NDE work in this project and that are related to enabling materials technologies:

- Showstoppers – increased availability of robust, low maintenance onshore turbines, as well as greater R&D into the development of increased reliability and availability of offshore turbines,
- Barriers – (i) integrated design tools for very large wind turbines operating in extreme climates, (ii) state-of-the-art laboratories for accelerated testing of large components under realistic (climatological) conditions, and (iii) standards and certification - development of design criteria for components and materials,
- Bottlenecks – development of component level design tools and accelerated finalisation of on-going standards,

FRP composite materials play an important role in the construction of wind turbines. The vast majority of wind turbine blades and the turbine nacelles are predominantly made from FRPs and composite sandwich structures. The strength-to-weight ratio of composites is the major advantage they have over other materials; their lighter weight means they need less wind energy to start their rotational momentum, which results in less mechanical and frictional loss in transferring this energy to the turbine. Minimising downtime, increasing structural reliability and improving design of wind turbine components manufactured from FRPs are key issues that are directly affected by the availability of suitable NDE techniques, procedures and standards.

Aim: The principal aim of the project was to address the lack of standards infrastructure for the non-destructive inspection of grades of FRP composite typically used in a number of applications across various energy sectors. To this end, the project aimed at the development of operational procedures for five NDE techniques to act as the pre-cursors of future standards.

How: The project developed operational procedures for microwave; active thermography; laser shearography, phased array ultrasonics and air-coupled ultrasonics NDE techniques by optimising the application of each technique using a range of bespoke reference and natural defect artefacts (RDAs and NDAs) designed and manufactured by the NMI partners. The RDAs and NDAs were constructed from a range of FRP composite materials used in energy applications and featured several classes of defects and damage typically encountered and required to be detected by industry. The operational procedures were then validated in collaboration with stakeholders through intercomparison, POD assessment and field trial exercises.

The project had the following objectives:

1. To design and manufacture suitable NDAs and RDAs that are representative of the materials and defects typically found in, and of concern to, the renewable energy (wind, wave, and tidal), oil and gas and transport sectors;
2. To develop operational procedures, drafted in the style of CEN and ISO standards, for: microwave, active thermography, laser shearography, phased array ultrasonics and air-coupled ultrasonics. The metrology objectives are to:
    i) Establish the limits of detection for each NDE technique;
    ii) Develop analytical techniques for accurately sizing defects for the five different NDE techniques;

iii) Compare the NDE techniques for different defect type using an objective POD benchmarking framework;

(iv) Advance the theoretical simulation of the inspection techniques;

3. To evaluate the POD methodology, based on modelling simulations with the aim of reducing the cost and time requirements of intensive experimental POD trials;

4. To validate and refine operational procedures via intercomparison exercises and field trials in collaboration with organisations from the renewable energy (wind, wave and tidal), oil and gas and transport sector supply chains. Defect artefacts will be inspected using the developed operational procedures.

3. Research results

The design and manufacture of suitable reference natural defect artefacts (RDAs) and natural defects artefacts (NDAs) that are representative of the materials and defects typically found in, and of concern to, the renewable energy (wind, wave, and tidal), oil and gas and transport sectors.

At the start of the project a very successful industrial survey was organised by NPL in consultation with BAM, PTB, CMI and REG(CEA) that established the material systems, components/structural elements and defect types (including size and location) that were most routinely required to be inspected, and those that presented significant challenges to NDE inspection. The survey had a total of 26 responses from organisations (predominantly European) across the oil & gas, renewable energy, lightweight transport, regulatory, material supplier and NDE equipment manufacturer sectors. From the findings of the survey, designs for 13 reference defect artefacts (RDAs) and natural defect artefacts (NDAs) were produced by NPL and BAM covering marine and automotive transport, renewable energy and oil and gas sector applications. Defect types included covered artificial delaminations, porosity, kissing bonds, fibre misalignment, pipe wall thinning (back-face drilled holes), core damage, impact delaminations and matrix cracking.

Table 1: Summary of designs for reference defect artefacts (RDAs)

Material/ sector	Name	Description
SE84LV Lightweight transport	2 off RDA_1a	• UD lay-up ($[0]_{16}$) ~ 5 mm thick • matt and gloss surface finishes • artificial delaminations of ∅3, 6, 12 & 25 mm • individual drilled holes ∅1, 2 & 3 mm, 3 x 3 arrays of ∅1 mm holes • 15° in-plane fibre misalignment (6, 12 & 25 mm square)
	RDA_1b	• multiple kissing bonds of ∅3, 6, 12 & 25 mm • two UD laminates ($[0]_8$) bonded with Redux 312 film adhesive
913G Lightweight transport	RDA_2a	• cross-ply ($[0/90]_{10s}$) ~ 5 mm thick • artificial delaminations; ∅3, 6, 12 & 25 mm • individual drilled holes ∅1, 2 & 3 mm, 3 x 3 arrays of ∅1 mm holes • 15° in-plane fibre misalignment (6, 12 & 25 mm square)
	RDA_2b	• multiple kissing bonds of ∅3, 6, 12 & 25 mm • two laminates bonded with Redux 312 film adhesive
Resin infused quadraxial glass fabric Marine/wind	RDA_3	• sandwich construction 450 x 650 mm • resin infused GFRP skins with PVC foam core; two flat regions of different core thickness (10 mm & 40 mm thick core) with smoothly varying transitions • top skin ~3 mm thick & bottom skin ~10 mm thick • artificial delaminations of ∅3, 6, 12 & 25 mm in skins • holes in core of ∅3, 5 & 10 mm at ¼, ½ and ¾ core thickness from back-face.
MTM®28 Oil and gas	RDA_4	• 10 mm thick pipe section (partial circumference) of MTM®28 (±55° lay-up) • artificial delaminations of ∅3, 6, 12 & 25 mm • drilled holes ∅5, 10 & 25 mm in pipe section; 1.5, 3 & 5 mm deep
PA12 GF60 Automotive	RDA_5	• UD lay-up ($[0]_{16}$) ~ 5 mm thick • artificial delaminations of ∅3, 6, 12 & 25 mm • individual drilled holes ∅1, 2 & 3 mm, 3 x 3 arrays of ∅1 mm holes • 15° in-plane fibre misalignment (6, 12 & 25 mm square)

In order to assess each NDE technique's robustness for accurately and consistently detecting a range of defects, RDAs were manufactured in which the defect sizes and locations were well defined and controlled. This necessitated the incorporation of artificially created defects including sealed polytetrafluoroethylene (PTFE) pockets mimicking delaminations, as well as individual and arrays of small diameter (1 mm) back-face drilled holes to represent discrete voids and porosity, respectively. The designs for the RDAs created are detailed in Table 1. Images of RDA_2a and RDA_3 are shown in Figures 1 and 2, respectively.

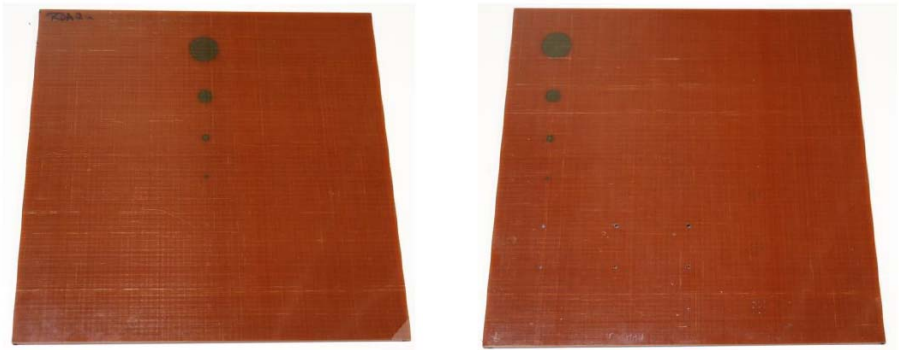

Figure 1: RDA_2a – 0°/90° 913 autoclaved GFRP: (left – top face, right – underside) showing back-face drilled holes and embedded artificial delaminations at different depths and sizes

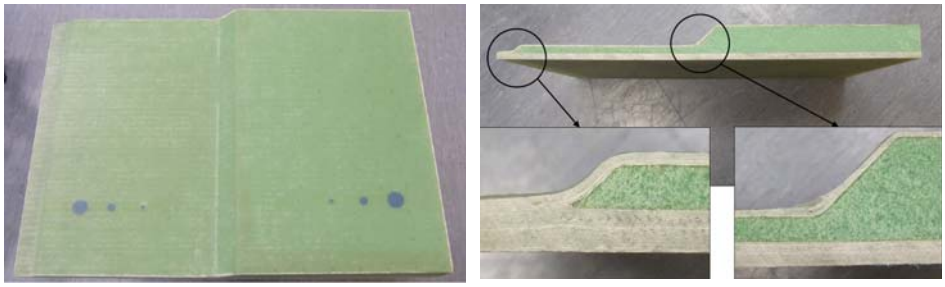

Figure 2: RDA_3 – Resin infused quadraxial GFRP: side view showing varying thickness double-sided foam construction (above) and details of associated transition regions and different skin thicknesses (below).

In addition, two types of NDA were designed and fabricated by BAM in which actual damage was created via tensile loading and low velocity impact. The NDAs are more representative of real defects than the RDAs as they feature multiple damage types (e.g. delamination, fibre fracture, matrix cracking) at multiple layers of unknown size, specific location and nature.

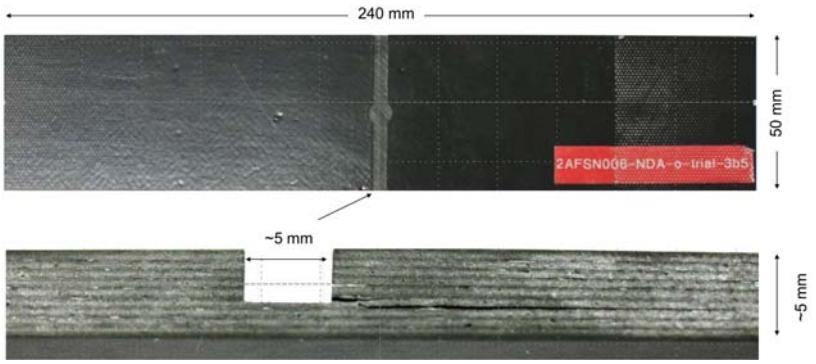

Figure 3: Example of 5 mm thick quasi-isotropic NDA with milled central notch and tension loaded to 32.1 kN: cut face (upper) and magnified side view showing delaminations created at the notch root (lower).

Figure 3 shows a rectangular coupon NDA with a notch milled across its width at mid-length. This design was used successfully to grow delaminations from the root of the notch in a controlled manner via tensile loading as shown in Figure 3. The second type of NDA is shown in Figure 4; panels of material supported on a base plate with a cut-out were impacted using a drop weight impact tower. For each material, two energy levels were used to create regions of impact damage of varying severity.

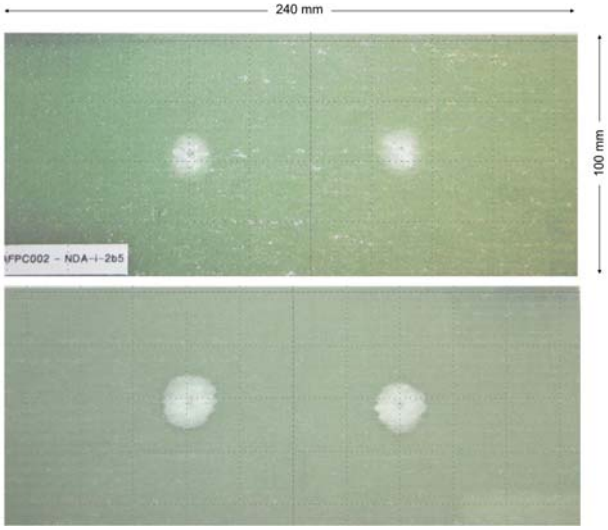

Figure 4: Example of 5 mm thick quadraxial NDA with 13 and 15J impacts showing evidence of surface indentation on the top face (upper) and extensive sub-surface damage zones on the rear face (lower).

NPL presented a paper entitled “Design and Manufacture of Reference and Natural Defect Artefacts for the Evaluation of NDE Techniques for Fibre Reinforced Plastic (FRP) Composites in Energy Applications” at the 19th World Conference on Non-Destructive Testing (NDT), in Munich, Germany in July 2016.

To provide the input material properties required for modelling approaches developed in the project for ultrasonic, microwave and active thermographic techniques, as well as optimising the practical application of these techniques, the elastic, dielectric, and thermal/optical properties for the materials used in the RDAs and NDAs were required, respectively. These were comprehensively characterised via measurements by the partners. A total of 5 FRP systems were used in the construction of the RDAs and NDAs.

Elastic properties

NPL had, in previous work, undertaken a full characterisation of the elastic properties for SE84LV carbon fibre-reinforced epoxy and 913 glass fibre-reinforced epoxy materials. The elastic mechanical properties of the remaining materials (Prime 20LV infused quadraxial glass fabric, MTM®28 glass fibre-reinforced epoxy and PA12 GF60 glass fibre-reinforced polyamide 12) were measured mechanically by NPL in tension (in-plane), compression (out-of-plane (Figure 5)) and shear (both in-plane and out-of-plane (Figure 6)) to provide the full complement of Young’s moduli, Poisson’s ratios and shear moduli.

Figure 5: Strain-gauged out-of-plane compression samples, all lateral faces prepared identically.

Figure 6: Notched and strain-gauged in and out-of-plane shear samples, front and back faces prepared identically.

Dielectric properties

The dielectric properties of the glass fibre-reinforced materials used in the RDAs were measured by NPL using the transmission/reflection line method. This involved placing a material sample inside a waveguide and measuring the complex scattering (S) parameters of the two ports with a vector network analyser (VNA). From this, the complex permittivity of the material under test was calculated. By measuring the properties in the three principal directions ('1' corresponding to the principal fibre direction, '2' the transverse in-plane direction and '3' the through-thickness direction), the anisotropic dielectric property dataset was determined. Dielectric characterisation measurements were made using a waveguide transmission cell method with rectangular aperture of cross-section 22.86 x 10.16 mm (Figure 7) in accordance with ASTM D5568. The measuring instrument used was a VNA model Rohde and Schwarx ZVB20 and the frequency range for the measurements was the microwave X-band 8.2 to 12.4 GHz.

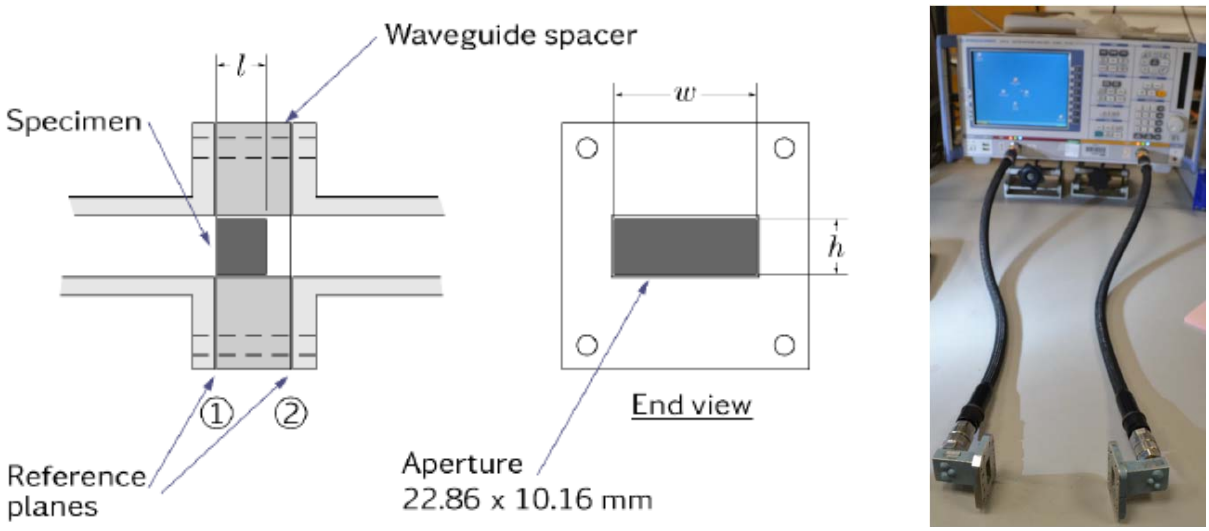

Figure 7: WG16 measurement cell, network analyser, flexible cables and waveguide transformers

The complex relative permittivity ($\varepsilon^* = \varepsilon' - i\varepsilon''$) was determined from measurements of complex S-parameters on the assumption that the specimens are non-magnetic. A result for complex permittivity was obtained by iteration from each of the four S-parameters (S11, S22, S21 and S12) at every measurement frequency. The well-known Nicolson-Ross-Weir algorithm was not used as it is prone to numerical instability. S21 and S12

(forward and reverse transmission) results were used in preference to the S11 and S22 results (forward and reverse reflection) because uncertainties are usually smaller.

Uncertainties of the complex relative permittivity measurements were evaluated from fixed dimensional uncertainties, and also estimates for the SD-parameter uncertainties and the phase instability of the VNA test-port cables. No allowance for the effect of gaps between specimens and the measurement cell were made, but these were expected to have negligible effect as the specimens were a close fit, and have fairly low permittivity.

An example of the dielectric properties measured in the '1' direction for a 0°/90° sample of 913 GFRP material is shown in Figure 8, whilst the mean values for dielectric constant at 10.5 GHz in the 1, 2 and 3 directions and for all non-conductive materials are detailed in Table 2. The reason the values were measured at 10.5 GHz is because this frequency corresponds to the lowest probe frequency used with the Evisive inspection equipment and could be measured because the appropriate waveguide was available at NPL.

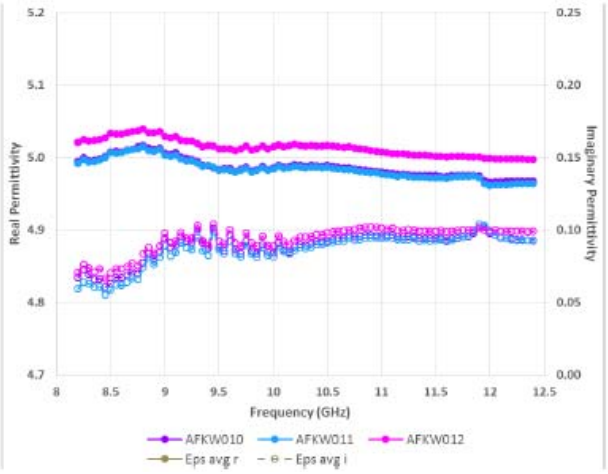

Figure 8: Dielectric properties in the '1' principal axis for 0°/90° 913 glass/epoxy laminate.

Material	Dielectric Property	Dielectric constant @10.5 GHz	Dielectric constant @24.1 GHz	Dielectric constant @34 GHz
0°/90° 913 glass/epoxy	d1	4.998	4.947 *(-0.051)*	4.926 *(-0.072)*
	d2	5.043	4.996 *(-0.047)*	4.976 *(-0.067)*
	d3	4.775	4.731 *(-0.044)*	4.713 *(-0.062)*
Resin infused quadraxial glass/Prime LV20	d1	4.774	4.714 *(-0.059)*	4.690 *(-0.083)*
	d2	4.788	4.730 *(-0.058)*	4.705 *(-0.083)*
	d3	4.528	4.506 *(-0.022)*	4.497 *(-0.031)*
±55° glass/MTM28	d1	4.724	4.694 *(-0.030)*	4.682 *(-0.042)*
	d2	4.984	4.946 *(-0.038)*	4.930 *(-0.054)*
	d3	4.653	4.615 *(-0.038)*	4.599 *(-0.054)*
UD glass/polyamide 12	d1	4.323	4.300 *(-0.023)*	4.291 *(-0.032)*
	d2	3.773	3.757 *(-0.016)*	3.750 *(-0.023)*
	d3	3.765	3.746 *(-0.019)*	3.737 *(-0.028)*

Table 2: Measured (10.5 GHz) and estimated (24.1 & 34 GHz) values of dielectric constant for VITCEA materials

For values of dielectric constant at the higher Evisive probe frequencies, 24.1 and 34 GHz, the measured data at 10.5 GHz was extrapolated numerically using the Lynch formula (Equation 1), which assumes the material response is characterised by the dielectric behaviour and that the loss is independent of the frequency. Here $\Delta\varepsilon' = \varepsilon_1' - \varepsilon_2'$ is the real permittivity at frequencies f_1 and f_2 respectively and *tan* δ is the dielectric loss tangent where $m \approx 1.5$ for frequency independent loss.

$$\frac{\Delta\varepsilon'}{\varepsilon'} = m \tan\delta \log_{10}\left(\frac{f_2}{f_1}\right) \quad (1)$$

All materials studied showed low loss characteristics indicating reasonable conformity to the assumptions specified in the Lynch formula. This suggested relatively little variation in the dielectric characteristics of the materials over the microwave frequency range. The average measured dielectric constant in each material direction at 10.5 GHz and the values determined mathematically for 24.1 GHz and 34 GHz using the Lynch formula are detailed in Table 2. The bracketed figures in Table 2 are the differences between the real part of the complex permittivity at 10.5 GHz and that calculated for the higher frequency. In all cases, the theory suggests a slight reduction in the dielectric constant with increasing frequency.

Thermal properties

Thermal diffusivity (α) and thermal effusivity (ϵ) are the key material properties describing heat transfer and which were required for the numerical models developed by BAM, as well as for quantitative analysis of data obtained from active thermographic inspections. Generally, these properties can be calculated from thermal conductivity λ, specific heat capacity c_p and density ρ of a material as follows:

$$\alpha = \frac{\lambda}{\rho C_p} \quad (2)$$

$$e = \sqrt{\lambda \rho C_p} \quad (3)$$

Thermal conductivity, specific heat capacity and density were measured by CMI, in all principal material directions for the 5 composite material systems studied, on specimens prepared by NPL. Subsequently, thermal diffusivity and effusivity were calculated from these measured properties.

The thermal conductivity of FRP specimens was measured via the Guarded Hot Plate (GHP) method. The measurements were carried out using CMI's Small Guarded Hot Plate (SGHP) apparatus which was built for this purpose (Figure 9). In principle, the SGHP apparatus is intended to establish a unidirectional uniform density of heat flow-rate within the specimen at steady-state conditions. The specimen is sandwiched between so-called hot and cold plates which maintain a temperature gradient across it and as a consequence, heat flow through the specimen occurs. The thermal conductivity λ can be then calculated as follows:

$$\lambda = \frac{Pd}{A\Delta T} \quad (4)$$

In equation 4, P is the electrical power applied to the hot plate metering section, d is specimen thickness, A is the measuring area, and ΔT is the temperature difference between hot and cold plates. The uncertainty of the thermal conductivity measurements undertaken via the SGHP technique was estimated to be 5%.

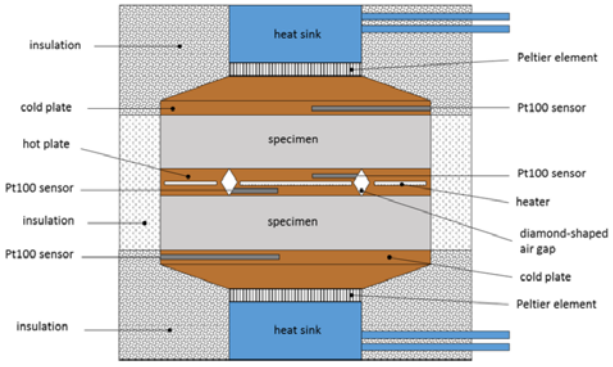

Figure 9: Schematic of CMI SGHP apparatus

Figure 10: CMI's adiabatic calorimeter

Specific heat capacity measurements were performed in an adiabatic calorimeter manufactured by CMI. The adiabatic calorimeter eliminates heat exchange between the specimen and its surroundings; therefore, the heat applied directly to the specimen should result in a temperature increase proportional to specimen heat capacity. The calorimeter consists of an inner measurement cell, a temperature-controlled radiation shield and an outer water-bath thermostated jacket. During measurement, the space between the measurement cell, radiation shield and outer jacket is evacuated to minimise heat transfer via convection and thermal conduction mechanisms. The adiabatic calorimeter used for the measurements is shown in Figure 10.

Heat capacity measurements were carried out using a step method and an approximate temperature increase rate of 2°C/hour. The resulting heat capacity values were determined based on measurements on the specimen and on the empty calorimeter (to determine the heat capacity of the inner measurement cell). The specific heat capacity c_p corresponding to the mean temperature $\bar{t}$ was calculated according to Equation (5):

$$C_p(\bar{t}) = \frac{P\frac{\Delta\tau}{\Delta t} - C_{cal}(\bar{t})}{m} \quad (5)$$

where P is the constant heating power applied to the inner cell for time $\Delta\tau$, Δt is the temperature difference caused by heating, C_{cal} is the heat capacity of the calorimeter determined by the calibration measurement,

and m is the mass of the specimen. The uncertainty of the specific heat capacity measurements was estimated to be 5 %.

The densities of the five materials were determined based on the measurement of specimen dimensions and mass. Measurements were made under laboratory conditions of 23 °C ± 1.5 °C and 50 % ± 20 % relative humidity. The uncertainty of the density measurements was estimated to be less than 0.5 %.

Table 3 shows calculated values of thermal diffusivity and effusivity for 5 FRP materials at room temperature. The estimated relative uncertainties for calculated thermal diffusivities and effusivities are 8 % and 4 %, respectively.

Table 3: Thermal diffusivity and effusivity data for 5 FRP materials calculated by CMI

Material	Lay-up	Orientation	Thermal diffusivity α / ($cm^2.s^{-1}$)	Thermal effusivity ε / ($J.m^{-2}.K^{-1}.s^{-0.5}$)
SE84LV, CFRP	Unidirectional	In-plane (1)	0.0210*	2114*
		In-plane (2)	0.0041	927
		Out-of-plane (3)	0.0034	852
913G, GFRP	0°/90°	In-plane (1)	0.0028	946
		In-plane (2)	0.0028	951
		Out-of-plane (3)	0.0023	859
MTM28®, GFRP	±55°	In-plane (1)	0.0025	884
		In-plane (2)	0.0028	945
		Out-of-plane (3)	0.0020	786
PA12, GFRP	Unidirectional	In-plane (1)	0.0026	919
		In-plane (2)	0.0023	867
		Out-of-plane (3)	0.0021	841
20LV, GFRP	Quadraxial	In-plane (1)	0.0028	928
		In-plane (2)	0.0028	937
		Out-of-plane (3)	0.0022	826

** - high values as measured for carbon fibre system in the fibre direction for a unidirectional laminate*

Optical properties

Material emissivity has a major influence on temperature measurement by thermal radiation, therefore knowledge of this quantity with the lowest possible uncertainty is essential for quantitative active thermography. For example, an uncertainty of 200 mK at 300 K at a detection wavelength of 4 µm requires an uncertainty in the emissivity of better than 0.01. To obtain the same temperature uncertainty at a detection wavelength of 8 µm (typical in field based experiments) the uncertainty of the emissivity has to be below 0.005. These uncertainties are currently the state-of-the-art for opaque materials with high thermal conductivities. For anisotropic composites with low and medium thermal conductivities, prior to the VITCEA project, these levels of uncertainty were beyond the state-of-the-art (currently about 0.02).

Using their Reduced Background Calibration Facility (RBCF) for emissivity measurements under vacuum (Figure 11), PTB demonstrated through measurements on a sample of SiC that the emissivity could be measured with a standard uncertainty (k=1) of better than 0.005 (Figure 12). Using this facility, PTB also made directional spectral emissivity $\varepsilon_\lambda(\lambda)$ measurements on the 5 FRP materials at 40°C and at observation angles of between 10° and 70° at 10° intervals with respect to the surface normal of the materials (Figure 13).

PTB designed a new sample holder for use with the RBCF (and associated methodology) to enable the simultaneous measurement of spectral emittance and the directional diffuse transmittance for partially transparent materials. The measurement scheme is based on a highly precise comparison of the spectral radiance of the sample and the spectral radiances of the two reference blackbodies at different temperatures. The intention was to use this new sample holder for measurements on FRP materials that might be partially transparent. Using their setup for diffuse reflectivity and transmissivity measurement, PTB made measurements of directional-hemispherical spectral emissivity and reflectivity for all 5 materials over the wavelength range 1 µm to 16.7 µm at a temperature of 25 °C. They then calculated the directional spectral emissivity from these measurements in the wavelength range 1 µm to 5 µm. Due to Plank's law, only a small amount of radiation is emitted at wavelengths shorter than 5 µm at 25 °C; an approach that is necessary to determine emissivities. The emissivity measurements in the range of 5 µm to 25 µm were then

performed using the RBCF setup for spectral emissivity measurement. All of the materials were found to be opaque in the range of 2.3 μm to 25 μm and only 3 materials showed significant transparency in the range of 1 μm to 2.3 μm. Therefore, it was discovered that the use of the new design of sample holder for simultaneous measurement of spectral emittance and the directional diffuse transmittance via a direct recording of emitted radiation was not required. For the new holder to have been used, either a higher but unrealistic temperature of over 250 °C (not suitable for the FRP materials used) or a transmittance at a higher wavelength than 5 μm would have been required.

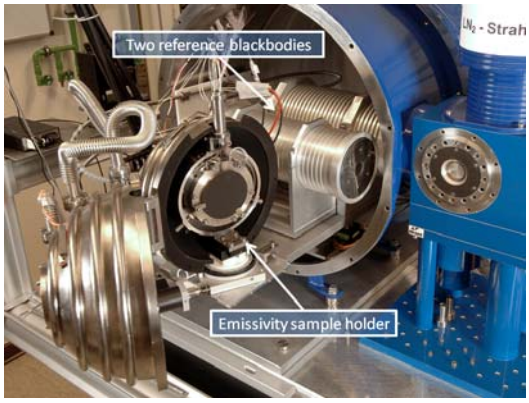

Figure 11: Setup for emissivity measurements under vacuum.

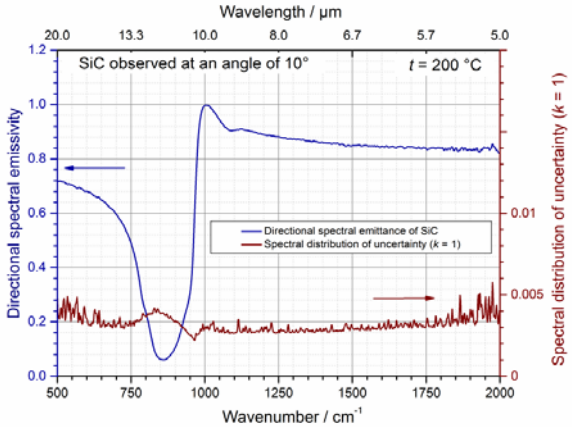

Figure 12: Directional spectral emittance of SiC measured at a temperature of 200 °C and for an angle of observation of 10° with respect to the surface normal. Additionally the spectral distribution of the standard uncertainty is shown.

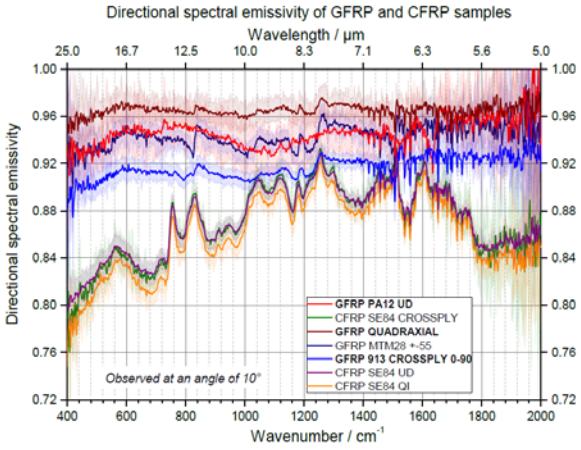

Figure 13: The directional spectral emissivity of all investigated GFRP and CFRP samples at a nominal temperature of 40 °C and for an angle of observation of 10° with respect to the surface normal. Standard uncertainty is shown as shaded area around the curves.

Due to the temperature limitation of the FRP materials studied, the measurements of directional-hemispherical spectral emissivity and directional-hemispherical spectral reflectivity in the range 1 μm to 5 μm were performed using an integrating sphere.

To develop operational procedures, drafted in the style of CEN and ISO standards, for: phased array and air-coupled ultrasonics; microwave; active thermography; laser shearography. Specific metrology objectives are to: (i) establish the limits of detection for each NDE technique; (ii) develop analytical techniques for accurately sizing defects for the five different NDE techniques; (iii) compare the NDE techniques for different defect types using an objective POD benchmarking framework, and (iv) advance the theoretical simulation of the inspection techniques.

Phased Array and Air-Coupled Ultrasonics

For phased array ultrasonic inspection, control of the beam propagating within an FRP composite is essential to achieve optimum inspection performance in terms of resolution and, consequently, to accurately size defects. Ultrasonic phased array probes are used to focus the beam via delay or "focal" laws, provided that those parameters are correctly calculated for the composite structure. These delay times are determined by the squint and beam angles required for the inspection scan, and these parameters enable the spatial characteristics of the expected ultrasound beam to be calculated. This is required to assess the measurement point distance and the distance of adjacent scanning tracks to cover the whole test volume and to optimise inspection speed. They also enable the ultrasound beam to be focussed within the reference artefact, improving the resolution of defects at different depths.

BAM developed a new measurement procedure using phased array ultrasonic inspection which took into account the anisotropy of the composite lay-ups used in the reference defect artefacts (RDAs). As details of the dimensions, defect types, elastic properties (measured by NPL) and lay-up of the RDAs were known, BAM were able to quantitatively determine the distribution of phase and energy velocities using the point source synthesis method. This enabled the specific test parameters for application of phased array inspection to be defined, including frequency, the single element size of the array and delay time distributions for excitation of transducer elements in either transmitting or receiving mode. For comparison to the BAM results, REG(CEA) also used their commercial CIVA® software to calculate the delay laws for each sample and for all of the ultrasonic transducers that BAM had studied.

BAM and REG(CEA) worked together on evaluating the limits of detection and sizing of the various defect types within the RDAs and NDAs using linear and matrix phased array methods featuring 16 and 60 2.25 MHz elements, respectively. Figure 14 shows the fixture that BAM used to enable probe manipulation and maintain water coupling between the probe arrays with the material under inspection, and Figure 15 shows ultrasonic scan images obtained from a matrix array inspection for RDA-2a.

Figure 14: Ultrasonic phased array inspection set-up and manipulator (water coupled)

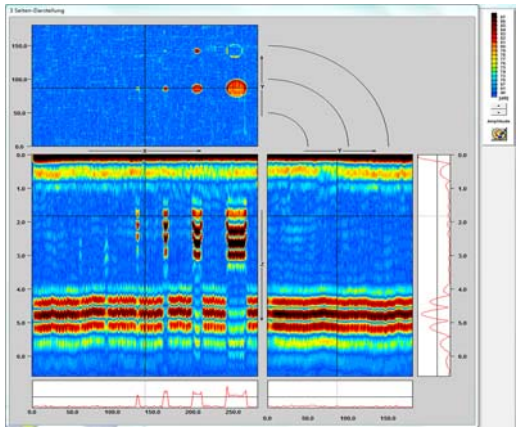

Figure 15: Matrix phased array scan results for RDA-2a

For each defect detected, BAM determined the signal to noise ratio (SNR) and the size of the defects, from the full width of the signal at its half maximum (FWHM). In addition, BAM calculated the detection ratio which was defined as the ratio of detected defects to the total number of defects present. BAM evaluated a Synthetic Aperture Focusing Technique (SAFT) signal processing algorithm in order to enhance the evaluation of measured data obtained using phased array inspection. However, results showed that use of the SAFT technique on ultrasonic B-scan data for RDA samples did not significantly improve the quality of data obtained. This was reasoned to be due to the size of the defects and the thickness of the material used in the RDAs.

Probes used in air-coupled ultrasonic inspection consist of transducers with impedance matching layers to minimise the detrimental effect of the high impedance mismatch between the transducer and the surrounding air. However, their main disadvantage is that the resulting signal-to-noise ratio (SNR) restricts the detectability of defects in the inspected component. BAM investigated the use of novel high SNR, focused, cellular polypropylene transducers (260 kHz) in order to improve the detection and resolution capability of non-contact, air-coupled ultrasound measurements. The set-up is shown in Figure 16. The results obtained using the novel air-coupled transducers were promising, as shown in Figure 17, however the drawback with this inspection technique is that results of this quality can only be obtained with a transmission arrangement, i.e. with the transmitting and receiving transducers on either side of the material under inspection. In practical inspection scenarios, it is not always possible to access both sides of a component, with one-sided access being more commonplace.

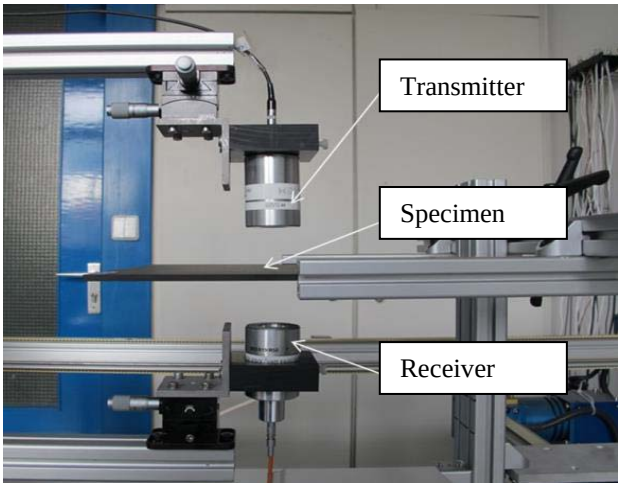

Figure 16: Ultrasonic air-coupled inspection set-up at BAM

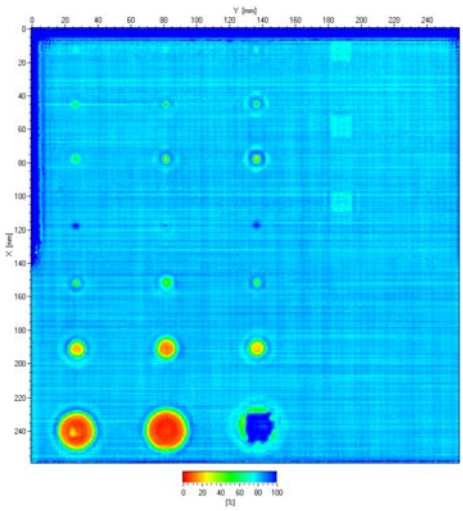

Figure 17: Ultrasonic air-coupled inspection results for RDA-2a (260 kHz)

For comparison to phased array and air-coupled inspections, BAM also inspected RDAs and NDAs with conventional ultrasonic pitch-catch immersion (5 MHz) and single transducer (2 MHz) transmit-receive techniques. For the immersion measurements, RDAs/NDAs were fully immersed in a water tank and scanned, whilst for the single transducer transmit-receive measurements, the transducer is in contact with the material via a Plexiglass block with water couplant sprayed onto the surface of the material via the arrangement in Figure 14. In general, similar values of detection ratio were found for detection of delaminations larger than 3 mm in diameter with the various techniques evaluated. The measured size and SNR values did not change significantly as a function of the defect depth.

REG(CEA), used two curved carbon fibre-reinforced plastic (CFRP) RDAs containing artificial delaminations, which were specifically designed and manufactured by NPL, to develop and validate modelling code to simulate the interaction of ultrasound waves and defects in thick and curved materials. REG(CEA) used a large set of validation cases of the developed code to ensure correct simulation of important parameters such as curvature, thickness, material homogeneity, attenuation and the nature of defects. The work gave REG(CEA) strong knowledge of the domain of validity of the proposed modelling tools.

Based on the best practice developed from the inspection of RDAs and NDAs using both phased-array and air-coupled inspection techniques, BAM produced draft operational procedures for both techniques.

Microwave Inspection

NPL used their Evisive x-y scanning system (Figure 18) to evaluate the effect of a number of parameters key to the microwave inspection technique. As the technique is only suitable for inspection of bulk non-conducting materials, only the GFRP RDAs were studied in this work. The parameters NPL evaluated included; (i) probe frequency (10, 24, 34 GHz corresponding to wavelengths of ~ 30, 12.5 and 8.7 mm), (ii) size of index increment (0.5, 1, 2, 4 and 8 mm), (iii) stand-off distance of the probe, (iv) spatial sampling rate, and (v) different backing materials e.g. metallic substrates.

The NPL scanning system consists of a rigid frame upon which a thick glass support plate is mounted. A single transducer operating as a transmitter-receiver (transceiver), mounted on a scanning bridge fitted with x (index direction) and y (scanning) linear position encoders, is scanned in a plane parallel to the specimen's surface. The transceiver consists of a transmitter diode that generates microwaves and projects them past two sensor diodes (channels A and B) which record the baseline field strength. The sensor diodes are separated by one quarter of a wavelength (for a given transmitting frequency), such that if one sensor detects a low or null signal then the other sensor should detect a higher signal, thereby increasing the sensitivity of the system. The microwaves emerge from a rectangular profile waveguide and then penetrate the test piece. At each interface at which there is a change in the dielectric constant in the material the microwaves will be reflected with modified amplitude and phase. For example, a delamination (i.e. air gap) will have a different dielectric constant from the parent material and hence it will reflect and transmit the microwave energy according to the differences in their dielectric constants.

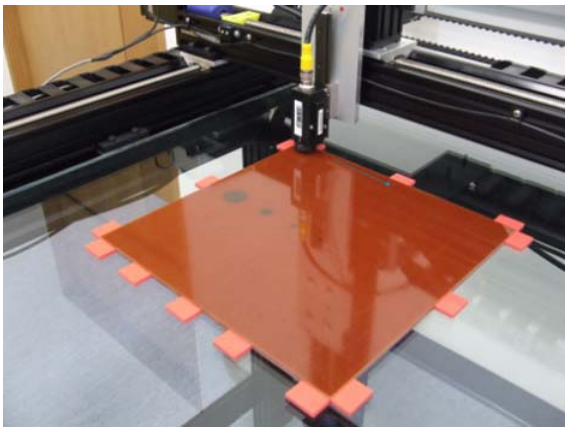

Figure 18: NPL's Evisive microwave inspection system

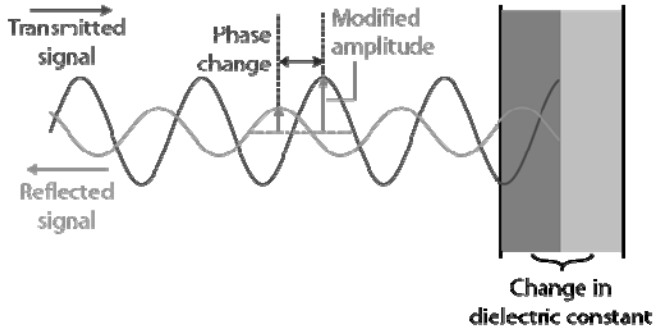

Figure 19: Schematic of phase change and modified amplitude due to reflection at an interface between materials of different dielectric constant

The signal voltage is determined from a pair of Schottky diodes located in the transceiver body. The voltage generated by each diode is a direct function of the magnitude of the microwave field the diode is detecting, but since the detector diodes are positioned in the transceiver body, the resultant microwave field detected is the summation of the outgoing (source) and incoming (reflected) signals. Therefore, there is a magnitude and phase component to the detector circuit response. The phase here is defined as the phase shift between the transmitted and superimposed received signals (Figure 19). The use of two detectors separated spatially enables a phase component to be calculated such that one channel is related to the cosine of the phase and the other channel is related to the sine of the phase. The measured signals are then amplified, digitised and converted into phase and magnitude images. The reflection method is applicable to cases where inspection access is limited to one side of a structure and is most sensitive to planar defects (e.g. delaminations) aligned normal to the axis of the microwave beam.

PTB used their expertise in electromagnetic modelling to simulate the interaction between microwaves and anisotropic composite material targets containing defects. The simulations, undertaken at 24.1 GHz only, replicated both the setup of the microwave inspection system used and the construction of selected RDAs. This enabled direct comparison with experimental measurements and allowed theoretical predictions of the detection of certain defect types. The simulation approach used initially focused on modelling each RDA using isotropic dielectric properties, but subsequently the models were further refined to include anisotropic properties measured by NPL for each material to ascertain how sensitive the simulations were to anisotropy. These subsequent simulations showed that only very small differences in the simulation results were observed, which is perhaps not surprising as the differences in dielectric constant properties in the three principal directions are small.

As expected, NPL observed better spatial resolution for detection of delamination and hole defects the higher the inspection frequency. At 34 GHz, all but the smallest diameter (3 mm) artificial delaminations were detected, as well as the 1 and 2 mm diameter individual back-face drilled holes and the 1 mm drilled-hole arrays. It was not possible to detect the in-plane fibre misalignment, a result explained by the fact that this type of defect has very little effect on the dielectric properties of the material.

NPL's evaluations of the effect of index increment showed that spatial resolution improved with decreasing index increment size. However, at small index increments (0.5 mm), striations were observed on the scan results which were initially thought to be an artefact of the scanning system or due to the fibre orientation in the surface ply. However, PTB were able to show via their simulations that this banding was actually due to superposition of lateral standing waves in the material most accurately sampled at small index increments.

Two different backing materials were evaluated by NPL; the first being a thick glass plate and the second a sheet of mirror finish stainless steel. It was found that detection of the artificial delaminations was in general clearer for inspections undertaken with a glass plate but the indications for back-face drilled holes (individual and array) were much clearer for inspections undertaken using a steel backing plate. This was due to increased local reflections of the higher amplitude reflected signal around the edges of the hole. In addition, for inspections using a steel backing plate, the amplitude of the striations at the edges and across the width of the RDAs at small index increments, were larger than when a glass plate was used.

As well as the methods for sizing defects included within the Evisive software, NPL evaluated the use of the FWHM technique via line profiles of amplitude signal versus position through detected defects.

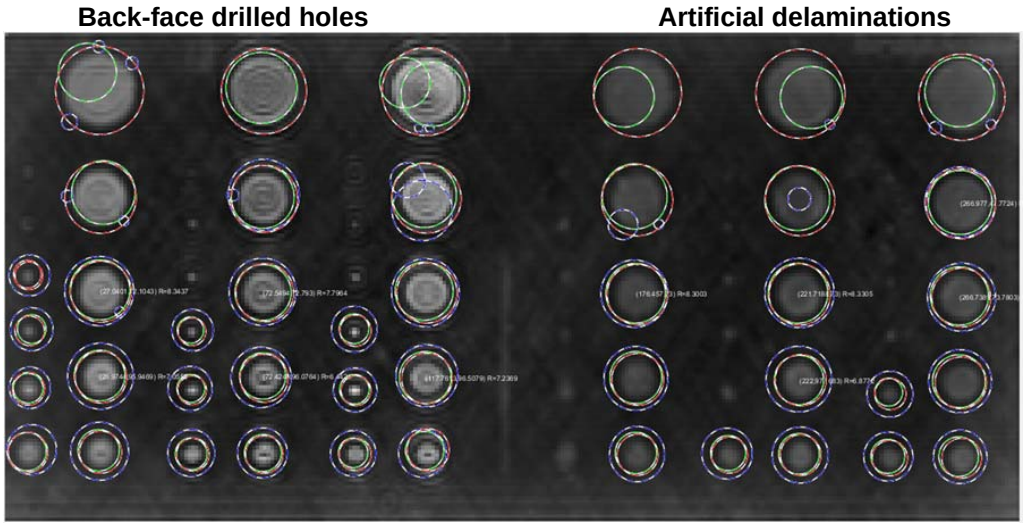

Figure 20: Circle parameters defined using Hough, Canny and Best fit algorithms, for back-face drilled holes and artificial delaminations detected in a GFRP RDA using microwave inspection

In addition, due to the noise observed around the edges of detected defects, particularly for back-face drilled hole defects where reflection of the microwave signal from the hole edges manifests in rings within and around the hole, a number of shape fitting algorithms (Figure 20, including Hough, Canny and best-fit) were evaluated to aid in the sizing of defects. NPL found that the best-fit algorithm gave the best results (Figure 21) for sizing of defects, however it is noted that this approach is only suitable for circular defects.

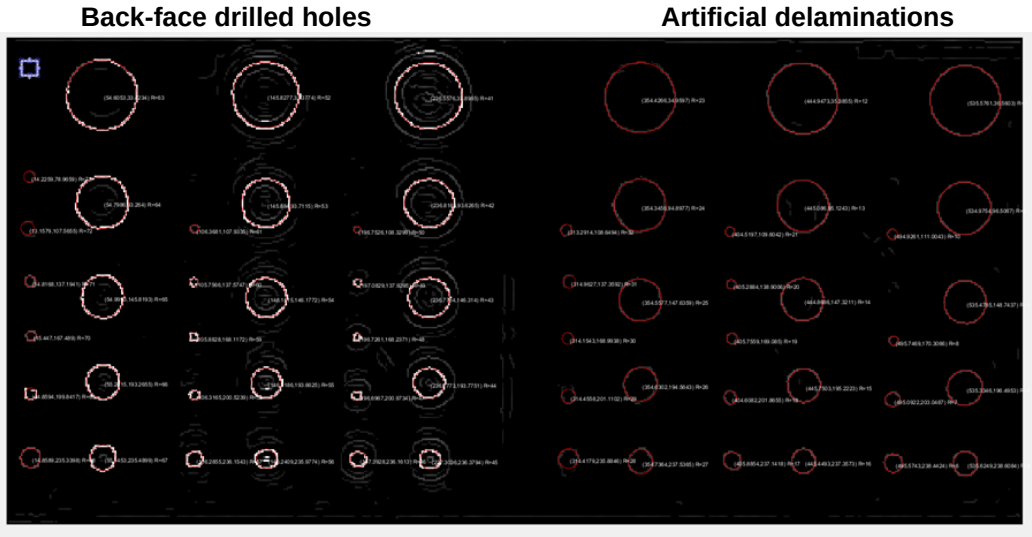

Figure 21: Identification and sizing of defects using best fit circle with intensity selection.

Through NPL's work, microwave inspection was shown to offer good detection capability for all defect types other than regions of in-plane misalignment, and there was excellent agreement PTB's simulated and NPL's experimental results. Artificial delaminations and back-face drilled holes of 5 and 25 mm diameter were able to be measured with a resolution of ±1 mm, with the smallest defect size detected being 4 mm diameter. The research undertaken by NPL and PTB resulted in a draft operational procedure for microwave inspection which was used in the assessments of POD intercomparisons and field trials.

Active Thermography

BAM led the optimisation and validation of active thermography techniques for full-field, fast and non-contact NDE. Initially BAM developed 2D and 3D models, using the thermal properties measured by CMI and emissivity data measured by PTB, to simulate non-stationary heat transfer in anisotropic FRP materials in order to optimise the reconstruction of active thermography data. BAM created finite element numerical models using COMSOL software to simulate pulsed thermography (PT), step heating thermography (SHT) and lock-in thermography (LT) inspection techniques for detection of the artificial delamination and back-face drilled holes in the RDA samples.

The models were optimised based on thermal measurements using the RDA samples. The following illustrates the approach that BAM took to model the pulsed thermography technique. With pulsed thermography (PT), an instantaneous heat flux is applied on the surface of the sample for a short period of time (typically a few milliseconds) and the heat diffusion in the material is monitored either in transmission mode (camera observing the temperature evolution at the rear side of the heat flux application) or reflection mode (camera observing the temperature distribution on the same side of heat flux application). After the heat source application, the sample is left under room conditions and the changes in the surface temperature are observed. In order to simulate the PT method, a three dimensional heat conduction model was developed using an instantaneous surface heat flux. The heat conduction in solids application module in COMSOL Multiphysics was used.

In contrast to previous research, in which an approximate heat flux distribution was used to model PT by choosing a constant heat flux value during the flash excitation period, BAM experimentally measured the temporal evolution of the high amplitude and short duration flash heating using a photodiode. The measured response is shown in Figure 22 and shows that the increase from zero amplitude to its maximum value and back to approximately 25 % of that peak takes about 5 ms, the rest of the 10 ms heat pulse shows a slow decrease towards the zero value. A function was fitted to the measured curve and used in the model.

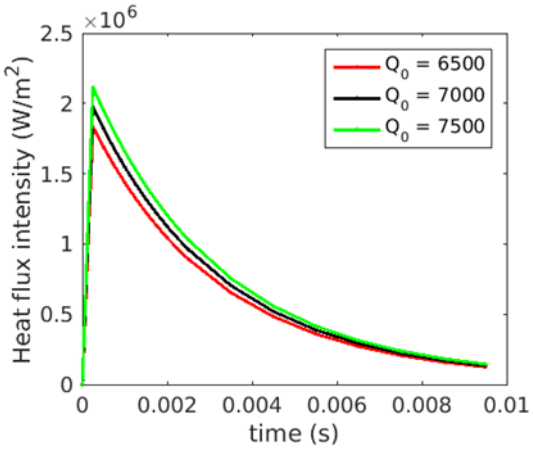

Figure 22: Temporal distribution of heat flux for different maximum powers calculated from experimental measurements on RDA-1a

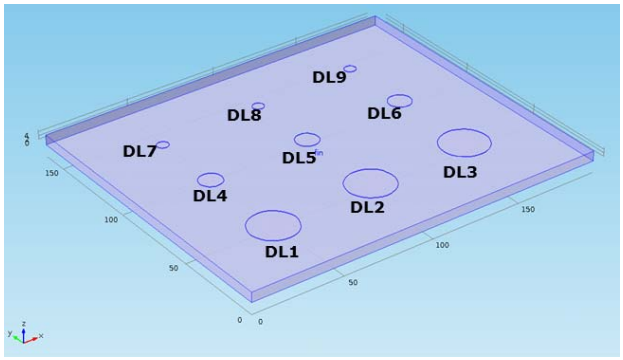

Figure 23: Model geometry of delaminations of various sizes and depth locations

Figure 23 shows the model geometry that BAM created for simulating the detection of artificial delaminations of 3 different diameters (6, 12 and 25 mm) at 3 different depths (0.59, 2.36 and 4.13 mm), and Figure 24 the simulated temperature evolution at different times after a 10 ms pulse heating of RDA-1a.

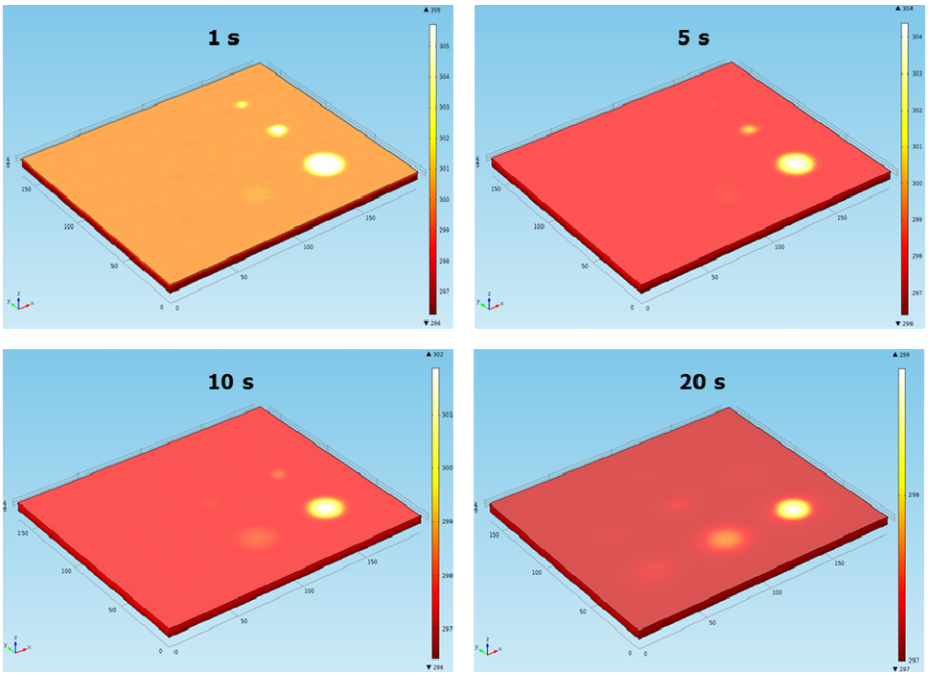

Figure 24: Temperature evolution after a 10 ms pulse heating of CFRP sample RDA-1a

Subsequently, BAM validated the modelling approach developed by simulating PT, SHT and LT inspection of several RDAs and comparing the predictions to experimental measurements. The validations were only undertaken on artificial delaminations and individual back-face drilled holes. The areas of fibre misalignment could not be detected using any variation of active thermography. BAM found that the agreement between model and experimental results was very good for all modes of heating. An example of the excellent level of agreement between simulation and experiment is shown in Figure 25 for time-temperature data comparison of PT inspection of RDA-1a.

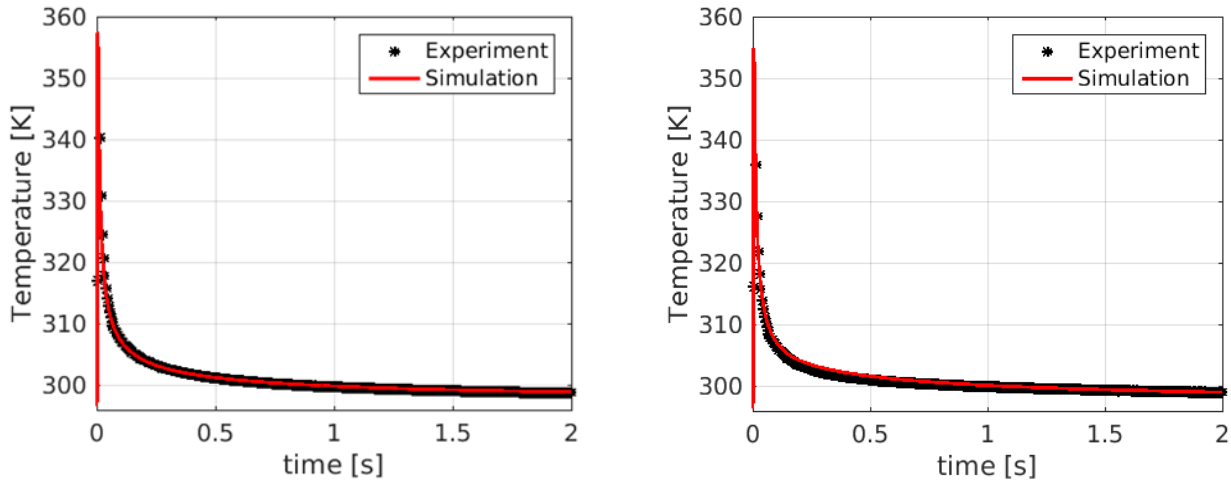

(a) (b)

Figure 25: Time-temperature data comparison of PT for RDA-1a sample (a) non-defective region (b) defect region (delamination: 25 mm diameter and 0.59 mm deep)

BAM used analytical models to optimise the measurement parameters for testing the RDAs with PT, SHT and LT thermography. The analytical calculations were based on the in-plane and out-of-plane thermal material properties measured by CMI. For all three variations of thermography only the reflection configuration of the experimental set-up was considered (i.e. heating sources and IR camera were positioned at the same side of the test specimen) to better represent inspection scenarios where access to the samples is restricted to one side. Through subsequent experimental inspections of various RDAs and NDAs, the practical application of the three thermographic techniques was optimised. For the optimised techniques, the SNR values were calculated for selected thermographs and phase images for each detected defect in RDA-1a (matt surface finish). Additionally, the SNR values of the thermographs of data recorded for selected NDA specimens were compared. BAM found that for RDA-1a, step heating gave the highest SNR values in the thermograms, whilst pulse thermography gave the maximum SNR values in the phase images for defects at shallow depths. For the NDA specimens, the highest SNR values in the thermograms for deeper defects were achieved with step heating, whilst the maximum SNR values for impact damage was achieved with flash heating.

BAM developed new methodologies to measure the size and depth of defects in RDAs by reconstruction of the defect size through an inverse approach using both pulsed thermographic data and the numerical finite element modelling described earlier. Three-dimensional (3D) anisotropic heat diffusion FEM models were used to consider the lateral heat diffusion effect. The inverse model includes two different analysis units; the first one is the defect depth correction unit and the second one is the simulation unit. The defect depth correction unit takes experimental data as input, calculates the depth and gives the output to the simulation unit. The simulation unit calculates the 3D heat diffusion and sends this information to the defect correction unit to calculate and compare the defect depth with the previously used value. A temperature comparison sub-unit is associated with the defect depth correction unit to check when a satisfactory comparison for the temperature evolution is reached after each iteration. This process of simulation and correction continues iteratively until the algorithm reconstructs the actual defect shape with the required precision.

BAM's work culminated in a draft operational procedure for active thermography which was used in the assessments of POD intercomparisons and field trials.

Laser Shearography

Defect detection using laser shearography (more accurately termed speckle shearing interferometry) relies on the optical measurement of relative changes in the surface topography of a component subjected to very low loads when compared to a reference condition. The technique has the advantages of being fast, non-contact and suitable for inspecting large areas, with portable, real-time and in-situ measurement capabilities. Detection capabilities of traditional NDE techniques are typically hampered by poor intrinsic material quality. They also struggle to distinguish critical defects from inherent material inhomogeneities, detecting all discontinuities, including those which may not be detrimental to the performance or ultimate strength of the material.

Laser shearography is different to the other NDE techniques studied in the mechanism employed to reveal flaws. The technique operates by measuring the direct mechanical response of defects to imposed stresses, unambiguously identifying material weaknesses. Laser shearography also readily lends itself to large assembled structures, which, in conjunction with actual service loading regimes, ensures critical defects, which are directly relevant to structural integrity and load-bearing capability, are detected rather than cosmetic imperfections.

NPL used their Dantec Q800 laser shearography system to assess the effect of a number of parameters key to successful application of the technique. Unlike the other techniques studied within the VITCEA project, laser shearography did not have a simulation element in the research undertaken.

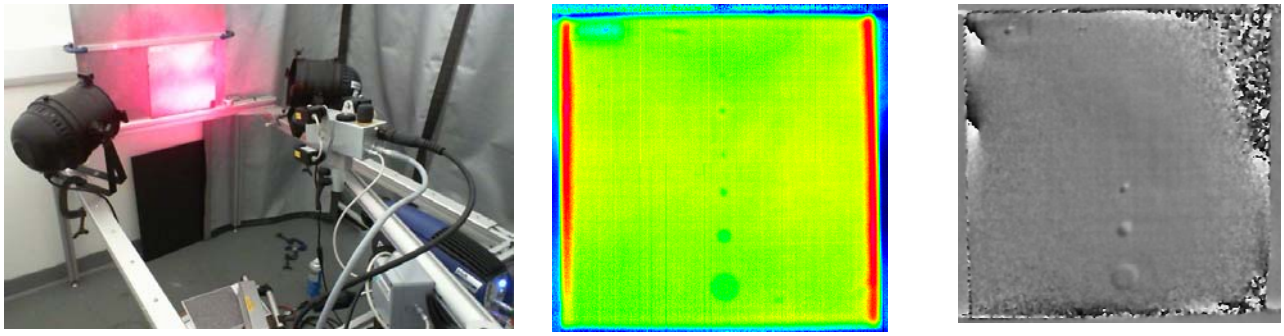

(a) (b) (c)

Figure 26: Feasibility of simultaneous laser shearography and lock-in thermography on RDA-2a; (a) equipment configuration, (b) phase image from lock-in thermography and (c) unwrapped phase shearogram

Initially NPL conducted a feasibility study to see if it was possible to simultaneously conduct laser shearography and lock-in thermography inspection using a single thermal excitation source. In the trials undertaken, 1 kW halogen lamps powered via a frequency generator were used to provide a modulated thermal stimulus to RDA-2a whilst both the laser shearography head and thermal camera (connected to a lock-in module) were arranged in-line and aimed directly at the RDA (Figure 26a). Figures 26b and 26c show the resulting lock-in thermography phase image and shearogram, respectively. The results were encouraging with both methods giving similar results, demonstrating capability of detecting near surface delaminations and some of the small diameter (3 mm) back-face drilled holes.

Through NPL's systematic parametric study of the laser shearography technique several key findings were found to be critical to achieving optimum and consistent results. The boundary conditions applied to the edges of the RDAs during inspection were found to have a significant influence on the resulting shearograms. When boundary constraints were not applied to samples fabricated from certain material types and lay-ups, then in-plane displacements caused by expansion of the material on thermal excitation caused decorrelation of images relative to the reference state. An example of this is shown in Figure 27 for inspections undertaken on the same unidirectional CFRP RDA, with and without boundary constraint. With no constraint, the thermal expansion of the material in the direction transverse to the fibre direction is large enough to completely de-correlate the data, whilst when the RDA was constrained, a good level of data correlation was observed. NPL found that for RDAs with multidirectional lay-ups, the application of boundary constraints was not as critical as fibre reinforcement in multiple directions, which effectively self-constrains the material.

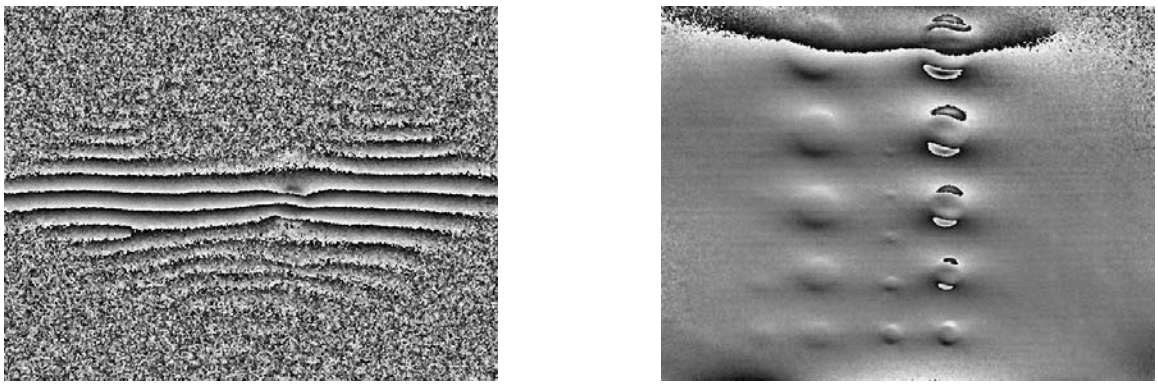

(a) (b)

Figure 27: Shearograms for unidirectional CFRP RDA (a) with no edge constraint showing high level of decorrelation and (b) with edge constraint showing little decorrelation

NPL evaluated the effect of the level of thermally induced stress on RDAs and found that whilst heating a sample for longer (i.e. increasing the temperature of the material) increased the level of heat transfer to deeper defects and thereby improving their visibility, the overall phase difference also increased resulting in image noise/decorrelation (Figure 28).

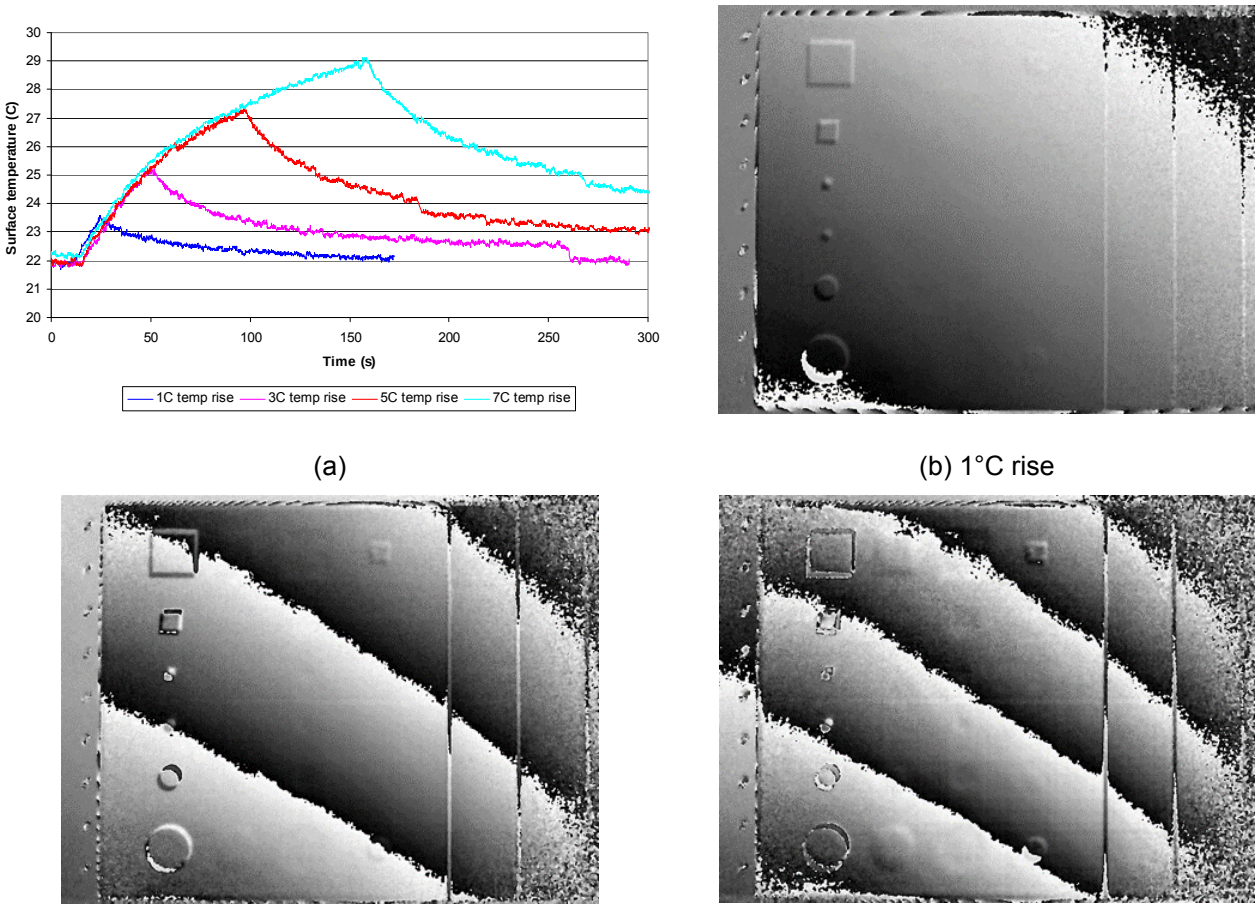

(a) (b) 1°C rise

(c) 3°C rise (d) 5°C rise

Figure 28: Effect of heating on defect detection and image correlation

NPL also found that for GFRP materials, with relatively high coefficients of thermal expansion (CTE), the greater thermal expansion for a given temperature increase compared to that of a CFRP material meant that the data de-correlated earlier, resulting in less depth sensitivity compared to CFRP materials.

Sizing of defects was highly dependent on the quality of phase difference shearograms, and so various noise reduction techniques (summing/averaging, filtering) were used by NPL to improve the definition of defect edges for size determination. The technique was found to have limited success for detection of feint or deep defects, e.g. defects with less than π variation in contrast (phase difference) or with small signal to noise ratios.

NPL produced a draft operational procedure for laser shearography based on the best practice developed during their parametric evaluation of the technique using the RDAs and NDAs.

Probability of Detection (POD) Benchmarking Framework and POD-RDAs

REG(CEA), NPL and BAM formulated a Probability of Detection (POD) benchmarking framework in order to evaluate the detection capability of each NDE technique using experimental, and where possible, simulated data. REG(CEA) led this work and used their expertise in POD assessment to construct a framework to enable POD assessments to be undertaken at a lower confidence interval thus reducing the required sample size. POD assessments are usually conducted at a probability of 90% and at a confidence level of 95 %, which would have been prohibitively onerous for the number of material, defect and NDE technique combinations within the project. To do this, REG(CEA) took into account the physical principles of each NDE technique and the typical format of data produced. From three candidate statistical approaches for POD determination, namely “29/29”, hit/miss and signal response analysis methods, an approach based on the signal response of each technique was chosen. The signal response methodology can be applied when the data fluctuate around a linear regression as shown in Figure 29 where the signal response is plotted as a function of the defect size.

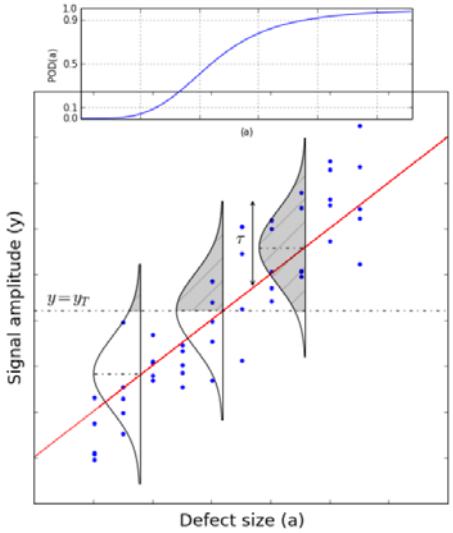

Figure 29: Example of how signal response methodology is used to determine POD (the POD is the fraction of the scatter density that is above the detection threshold)

POD assessments were undertaken on a subset of the materials and defects that featured in the RDAs described earlier. The two materials selected were SE84 CFRP and MTM28® GFRP and the defects chosen were artificial delaminations and back-face drilled holes. NPL designed and manufactured two RDAs, one of each material and featuring both defect types, which were subsequently termed POD-RDAs. In order for the POD approach to be valid, sufficient numbers of defects and of appropriate sizes needed to be incorporated into the POD-RDAs. Therefore, guidance was taken from REG(CEA) in which POD curves were calculated from ultrasonic data from initial inspections on RDAs. Subsequently, the defect size range was increased significantly from those used in the RDAs, to ensure that the POD-RDAs featured defects that were too small to be detected ranging through to defects that were large enough to guarantee detection. Each POD-RDA (Figure 30) featured 13 artificial delaminations at three different depth locations, ranging in size from 1 mm to

40 mm diameter, as well as the equivalent configuration of back-face drilled holes. Therefore each POD-RDA featured 39 artificial delaminations and 39 back-face drilled holes.

(a) (b)

Figure 30: SE84 CFRP POD-RDA (a) back-face image and (b) ultrasonic C-scan (5 MHz, 3" focussed probe)

To evaluate the POD methodology, based on modelling simulations with the aim of reducing the cost and time requirements of intensive experimental POD trials;

One of the objectives of the VITCEA project was to advance the state-of-the-art of modelling techniques for phased array ultrasonics, microwave inspection and active thermography such that data for POD analysis of the POD-RDAs could be generated via simulation. With the exception of phased array ultrasonics, it was not possible to use these models to generate simulated data though advances in modelling capability for microwave and thermography were made by BAM, PTB and NPL. Hence, the evaluation of the POD methodology (developed by REG(CEA), NPL and BAM) was performed using simulated data to supplement measured data from experimental POD assessments undertaken by BAM for the phased array technique only.

REG(CEA) took experimental POD data generated by BAM for phased array inspection of both CFRP and GFRP POD-RDAs and generated POD versus size of defect curves (delaminations and back-face drilled holes) in order to identify the size of defect that could be detected with a POD of 90 % within a 95 % confidence bound $a_{90/95}$. An example plot of this data is shown in Figure 31a.

(a)

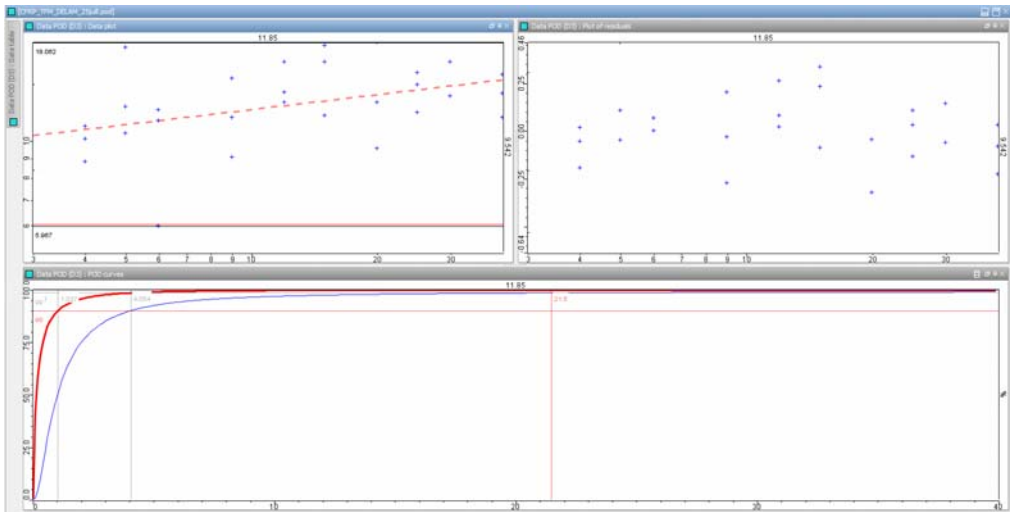

(b)

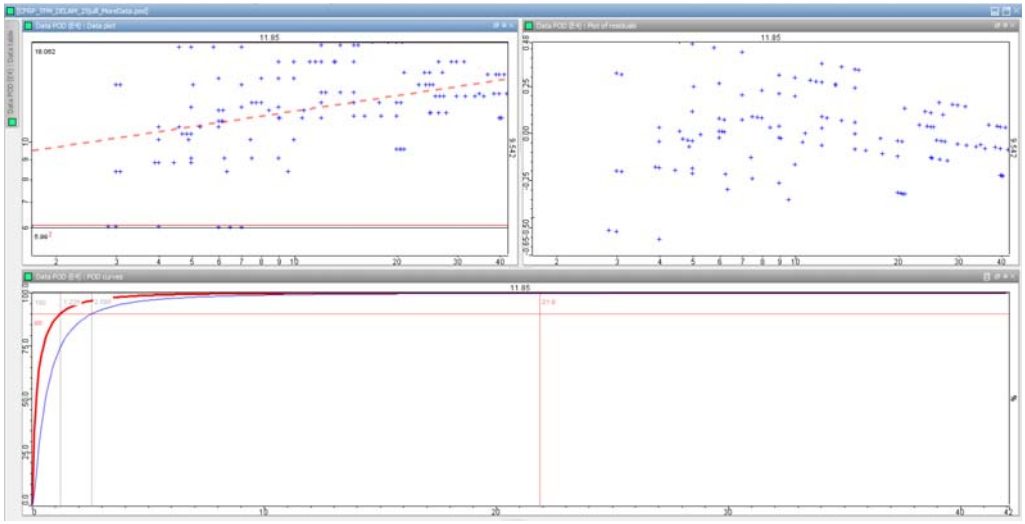

Figure 31: Log-Log plot of POD 90/95 for phased array ultrasonic inspection of delaminations within CFRP POD-RDA (a) experimental data only, (b) experimental data supplemented with simulated data

REG(CEA) then used their CIV software to simulate data which were then combined to the experimental data-set and replotted (Figure 31b). From the experimental data only, the value of $a_{90/95}$ was found by REG(CEA) to be 4.05 mm, whilst the combined simulated and experimental dataset reduced this value to 2.58 mm. REG(CEA) were able to conclude that the phase array datasets fitted the POD model assumptions that were built into the POD benchmark design.

REG(CEA) demonstrated that the principle of using simulated data to supplement or replace experimental data is feasible provided that the modelling capability exists for a given NDE technique.

To validate and refine operational procedures via intercomparison exercises and field trials in collaboration with organisations from the renewable energy (wind, wave and tidal), oil and gas and transport sector supply chains. Defect artefacts will be inspected using the developed operational procedures.

The initial project plan was to validate and refine the draft operational procedures through intercomparison exercises, experimental POD assessments and field trials. The intercomparisons for each NDE technique that were planned at the start of the project were combined with the experimental POD assessments (renamed POD intercomparisons) involving project participants and stakeholders. This was a decision made at the mid-point of the project on advice given by the mid-term review panel.

BAM and NPL used their respective industry contacts to invite at least two stakeholder organisations (per NDE technique) to take part in experimental POD assessments using the two POD-RDAs as inspection samples. A total of ten industry stakeholders took part in the assessments, which was considered to be a significant level of participation when the nature of the task required of participants is considered. NPL formulated a test protocol for the POD assessments that was sent out to each participant, in turn, along with the POD-RDAs and draft operational procedures. Participants were requested to perform two inspections of the supplied POD-RDAs according to the supplied operational procedure to provide the statistical dataset required for POD analyses. Between each inspection, they were asked to reset the NDT system and settings. It was also communicated that having a different user following the procedure for the second trial would prove useful. Participants were asked to send back results in the form of scan images as well as measured sizes of those defects detected. As participants took part in the POD assessments out of good will, it was not always possible for them to send back all of the data requested due to other constraints on their time.

Each partner collated data from their respective participants and any further data interpretation or reduction was performed prior to sending the data to REG(CEA) for POD analysis. The data sent to REG(CEA) was in the format of signal to noise ratio versus measured defect size. For all techniques apart from laser shearography, for which the quantity of data returned by participants was insufficient, it was possible to produce POD curves and values of $a_{90/95}$ for artificial delaminations and back-face drilled holes. Figure 32 shows a comparison of the $a_{90/95}$ values for phased array ultrasonics (PAUT), air-coupled ultrasonics

(ACUT), microwave (μW) and thermography techniques for artificial delaminations and flat-bottom holes. The numbers of data points for each technique correspond to individual data-sets provided by participants that were suitable for assessment.

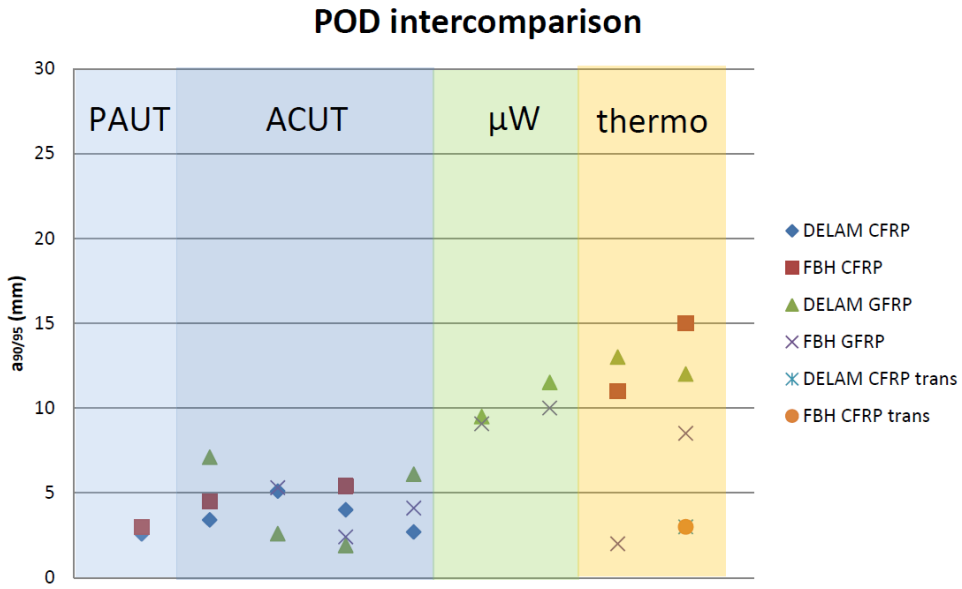

Figure 32: Final POD intercomparison results for POD-RDA specimens for ultrasonic, microwave and thermography inspection techniques

The ultrasonic results were observed to be generally better than for other techniques, however REG(CEA) reasoned this to be due to the larger data-sets analysed with the inclusion of simulated data. Despite limited data for the POD assessments, REG(CEA) concluded that sufficient data was measured and analysed to give a meaningful POD intercomparison of the four techniques.

In addition to the POD intercomparisons, selected field trials were undertaken by NPL and BAM. Although it was initially planned to perform inspection trials on operational components in the field, the complexity of arranging access to such assets and utilising principally laboratory inspection systems meant the decision was made to conduct trials on samples and components containing real defects that were sourced from industry stakeholders. These inspection trials were undertaken in a laboratory environment.

NPL investigated the use of microwave inspection for detection of de-bonds or delaminations between a metal substrate (representing an oil and gas pipeline) and a quadraxial glass over-wrap repair system (Figure 33). Composites are used in the oil and gas industry for the repair of corroded pipe-work and pipelines, and to rehabilitate pipe-work systems suffering either internal or external corrosion. They are also applied to pipe systems that are leaking, i.e. a through pipe-wall defect, usually caused by excessive wall thinning. Recently, there has been much interest in the application of various inspection techniques for checking for de-bonding between the metal pipe and the repair laminate. Typically this has been performed by organisations in the oil and gas industry using samples representative (Figure 33b) of real repair scenarios. NPL performed inspections on model samples supplied by ESR Technology Ltd and WTR. The samples were pressure tested to deliberately de-bond the GFRP over-wrap repair via the hole drilled through the metal substrate.

(a) (b)

Figure 33: Oil and gas composite over-wrap repairs: (a) as applied to piping and (b) model sample for laboratory inspection case studies

NPL scanned the sample using a 34 GHz microwave probe at an index increment of 0.5 mm in accordance with the operational procedure that had been developed earlier in the project. The results were promising and clearly showed the extent of de-bonding around the central PTFE insert which was used to initiate the de-bond (Figure 34). It would not have been possible to obtain this quality of result with ultrasonic techniques as the inherent porosity levels in this quality of composite would attenuate ultrasound significantly. In addition, the thickness of repair laminate would have meant that success with the use of thermographic techniques would have been limited.

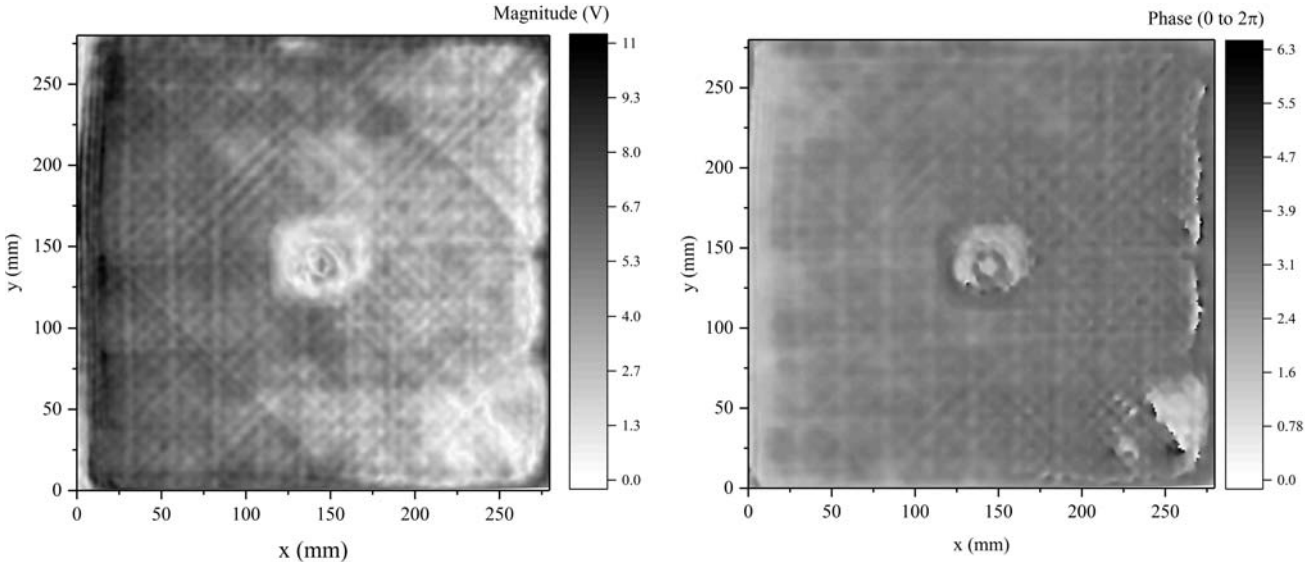

(a) (b)

Figure 34: Microwave inspection result for composite over-wrap repair; (a) magnitude and (b) phase

This same sample was also inspected using laser shearography. The sample was heated using two radiant lamps, imaged using a variable zoom lens at approximately 1.5 m from the specimen surface at a zoom of 20 x. Measurements were performed with a shear angle of 0º with an offset of 3.05 mm, in accordance with the operational procedure that had been developed earlier. The results were promising and, despite decorrelation occurring due to the high thermal expansion of the GFRP overwrap and the underlying metal substrate, clearly showed the central delamination and the break-out point at the upper boundary of the plate (Figure 35), as well as highlighting the fibre format within the composite. It is likely that a pressure-based

excitation method would have been even more definitive since this would be solely reliant on mechanical response rather than the somewhat more complex thermo-mechanical response.

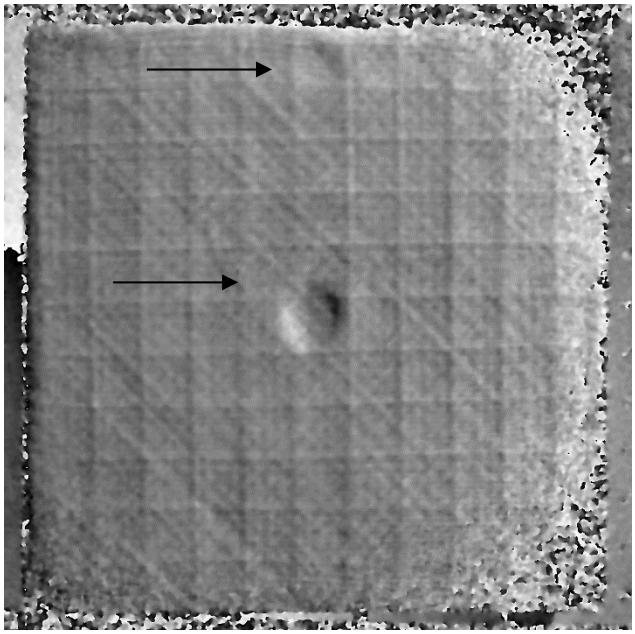

Figure 35: Laser shearography inspection result for composite over-wrap repair; phase map displayed with 3 pixel smoothing and 100 pixel high pass filter, central delamination, fibre format and upper boundary breakout zone visible

BAM applied thermographic techniques to sections of wind turbine blade constructed from a number of materials including GFRP, wood and adhesives. Figure 36 shows a schematic of the blade as well as images of one of the sections extracted from a region close to the beams in the centre of the blade.

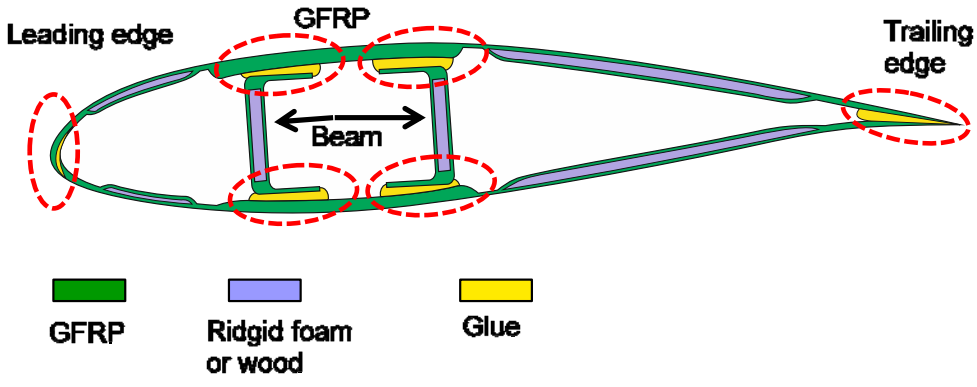

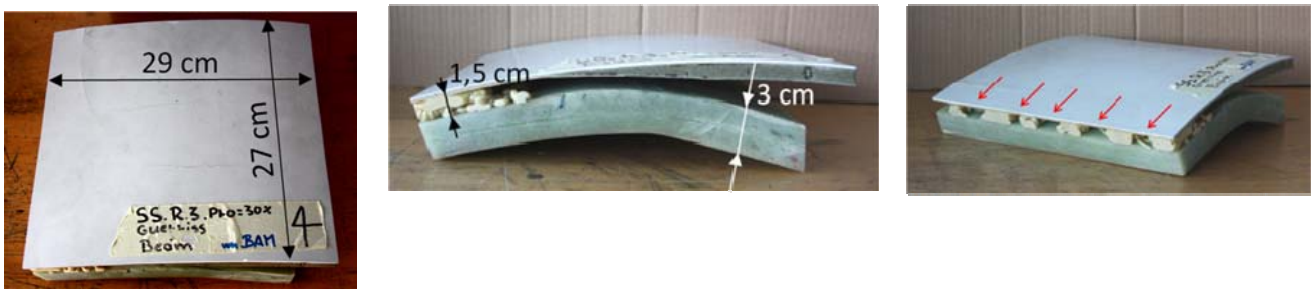

Figure 36: Schematic drawing of the cross-section of a wind turbine blade and images of section cut from a region near to the beams in the centre of the blade

For the section shown in Figure 36, the inner structure is curved and has a thickness of about 3 cm. Bonding between the beam and outer shell was not performed consistently as it is clear that the bond-line consists of several beads of adhesive rather than having continuous coverage over the bonded area.

BAM performed inspections with active thermography using three excitation techniques: pulse excitation, lock-in excitation and step heating with an infrared radiator. The experimental set-ups for pulse and lock-in excitation are displayed in Figure 37.

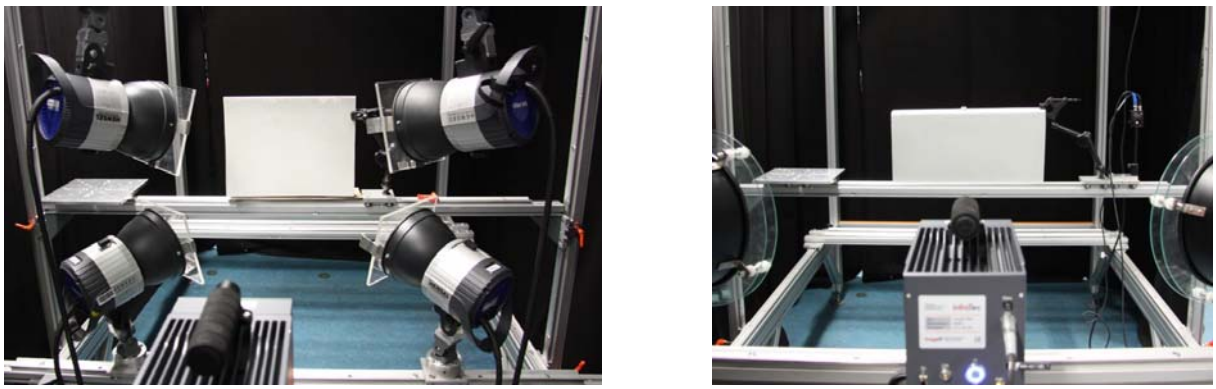

Figure 37: Experimental set-up for flash excitation (left) and lock-in excitation (right).

In Table 4, the results obtained for the wind turbine section are summarised. For each excitation technique, BAM calculated phase images either from the thermograms recorded during cooling down (after pulse or step excitation) or recorded during the lock-in excitation. BAM obtained very good inspection results with all thermographic methods. In the phase images of pulse excitation at 0.01 Hz as well as for step excitation, the structure of the adhesive beads on the left-hand side were easily identified. The vertical foam edge can be seen clearly in all of the phase images. The horizontal lines shown in all phase images with lower frequencies (0.01 and 0.005 Hz) correspond to the infusion channels of the foam. In the top left part of the sample, delaminations around a crack are visible in the phase images at higher frequencies (0.05 and 0.01 Hz).

Table 4: Active thermography results obtained for wind turbine blade sample

	Flash excitation	Lock-in excitation	Step excitation
0.05 Hz	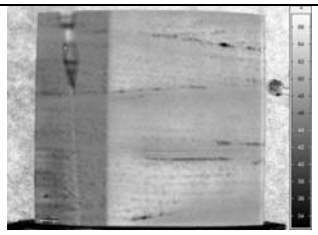		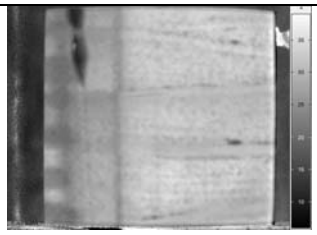
0.01 Hz	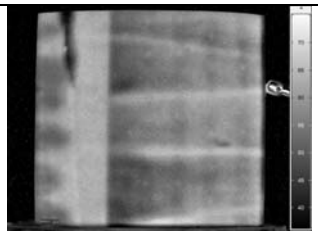	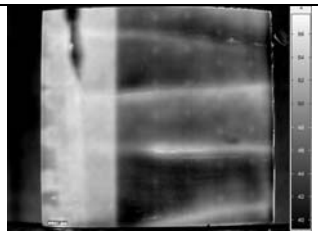	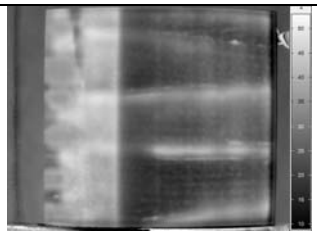
0.005 Hz			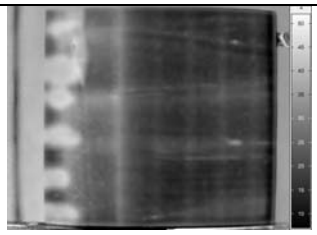

Following completion of the POD intercomparisons and field trials, BAM and NPL updated the draft operational procedures for each technique, taking into account any feedback received from stakeholders that had used them during the validation exercises. All of the procedures were written in the form of an ISO standard such that in future work the procedures could form the basis of standards or best practice guidelines for FRP inspection.

4. Actual and potential impact

Dissemination activities

The project created a large stakeholder community with more than 67 members across the EU and the US. The community comprised of representation from across the entire supply chain including FRP composite material suppliers, designers and end-users of both FRP products and NDE equipment, regulatory bodies, research and technology organisations (RTOs) and academia. This wide range of representation was specifically targeted to maximise exposure of the consortium to the industrial requirements that needed to be addressed, thus ensuring the project delivered the most useful results and to ensure that dissemination of project outputs had a wide, varied and appropriate audience.

A project website (http://projects.npl.co.uk/vitcea) was set-up at the start of the project and updated regularly, with project events and news.

NPL published articles in two trade journals; ‘EU Researcher Magazine’ during April 2016 and ‘Adjacent Government’ during August 2016. Both articles, which were accessible on-line as well as being in hard copy, highlighted the VITCEA project aims and research. These articles were aimed at a more general readership so that a wider audience could be reached.

Stakeholder Engagement / Workshops

At the start of the project a very successful stakeholder survey was undertaken in which 26 detailed responses were received by the consortium. This exercise was designed to confirm that the material formats, defect types, sizes and locations, processing routes and generic constructions chosen by the consortium were of direct relevance to industry. The consortium arranged a highly successful 1st VITCEA workshop held at BAM on the 17th February 2015. A total of 10 industry presentations were given by stakeholder organisations. In total 48 attendees were present at the meeting; 34 at BAM and 14 online from the US, UK, France and Germany. An overview of the VITCEA project was presented by NPL and the stakeholder presentations provided excellent real-world context for the VITCEA research.

A 2nd stakeholder workshop was held towards the end of the project at NPL with all participants present and external visitors from ESR Technology, National Composites Centre, Exova, University of Surrey, Evisive and University of Manchester. The consortium presented the main research findings from VITCEA as well as details of the finalised operational procedures developed.

Technical Dissemination

The technical dissemination of the project took place through 3 posters and 23 presentations at a number of major conferences including Quantitative InfraRed Thermography (QIRT) 2016, the 19th World Conference on NDT (WCNDT-19), the 17th European Conference on Composite Materials (ECCM-17), the 20th International Conference on Composite Materials (ICCM-20), the European Conference on Thermophysical Properties (ECTP 21), Temperatur 2017, the 11th European Conference on Non-Destructive Testing (ECNDT-11), International Symposium on Fatigue Design and Material Defects (FDMD) and the 19th International Conference on Photoacoustic and Photothermal Phenomena. Papers for 9 of the conferences have been included in conference proceedings.

A total of 3 peer-reviewed publications were published during the project, with at least 3 more to be submitted after project completion. The papers cover various aspects of the project and demonstrate the success and outputs achieved.

A number of technical presentations were also given to industrial and academic stakeholder groups including 5 to NPL's Composites, Adhesives and Polymers Industrial Advisory Group (IAG). Presentations to this group, which has an attendance of around 30 members, covered the design and production of RDAs, NDAs and POD-RDAs, laser shearography and microwave inspection.

At the start of the project, NPL were invited to become members of the newly formed Composites Group of the British Institute for Non-Destructive Testing (BINDT). BINDT is a UK technical institute that feeds into composites standards and regulation via the British Standards Institution (BSI) and ISO. A standards slot was added to the standing agenda of this Group and an overview of the standards work within VITCEA was given by NPL at the 6-monthly meetings. A presentation of the VITCEA project was given by NPL to the NDE Defect Library engagement workshop at the National Composites Centre (UK) in January 2015.

BAM presented at the Carbon Composite e.V. (CCeV): Seminar of WGS NDT, Adhesive Technology in Germany, 3rd July 2015. CCeV is an association of companies and research institutes which covers the entire value chain of high performance fibre reinforced composites. CCeV links research and business in Germany, Austria and Switzerland.

Standards

Standards for the inspection of composites are not well developed. The project has moved the standardisation of NDE-FRP composites specific techniques forward significantly with 7 contributions to standards / standards bodies engaged with during the project by NPL, BAM, PTB and CMI.

BAM successfully engaged with 2 standards working committees: TC138 (Non-destructive testing, CEN) and NMP Materials Testing (DIN). In each case, an overview of the aims and objectives of the VITCEA project was presented to the WG at meetings in Berlin. In February 2016 PTB presented details of their emissivity measurements and results to the EURAMET Technical Committee for Thermometry (annual meeting in Malta 23rd-26th February). NPL disseminated progress made in the development of reference defect materials to ISO TC61/SC13/WG2.

NPL coordinates composites standards developments through the Versailles Project on Advanced Materials and Standards (VAMAS). The main objective of VAMAS is to promote innovation and adoption of advanced materials through international collaborations that provide the technical basis for harmonisation of measurement methods, leading to best practice and standards. In May 2015 an overview presentation of the VITCEA project was given to VAMAS delegates by NPL at the 41st Steering Committee meeting as well as details of the RDA and NDA design and manufacture. During the afternoon, a lab tour was given during which the microwave and laser shearography techniques were described. VITCEA work was also presented at the 42nd VAMAS Steering Committee meeting in Mexico.

An overview presentation of the VITCEA project was given by NPL to the Regulations, Codes and Standards (RCS) Working Group of the UK Composites Leadership Forum. This is a UK industry body that feeds into composites standards and regulation via BSI and ISO.

Training

As part of the training activities within VITCEA, NPL produced an e-learning module for microwave inspection that is based on the operational procedure developed within the project. The module is entitled 'Microwave NDT for Composites Explained' and is a live module. A lecture, entitled "NDE of Composite Structures" was given twice during the VITCEA project as part of Surrey University's "Introduction to Composites" short course. The lecture was attended by ~30 delegates who were mainly from the scientific community, being either Phd or EngD students or from public research organisations. In addition to the lecture, two practical demonstration sessions were given by NPL; one on the use of laser shearography and the other on the application of passive thermography for damage detection during fatigue loading of FRP composites.

BAM held a 3-day training course on thermographic and ultrasonic inspection at the BAM site in Berlin. The course was well attended by over 20 participants from industry.

Early Impacts

All participants in the project have developed a number of new and enhanced Metrological Capabilities, which are now available for both further collaborative research or for commercial use by end-users' asset owners, end-users, designers and NDE communities involved with the use of FRPs in energy applications in the renewable, oil and gas and lightweight transport sectors. The key project outputs that will be exploited will include:

- The creation of 13 reference materials, sector specific RDAs, NDAs and POD-RDAs, including design and production methodologies. These are freely available for stakeholders to borrow and use to validate optimised application of various NDE techniques. Whilst RDAs and NDAs have been produced previously by other research groups, the level of characterisation performed on the materials from which the artefacts created in the VITCEA project were fabricated was unprecedented and demonstrates the expertise now held within the partners.
- The consortium formulated five validated operational procedures for ultrasonic (phased array, air-coupled), microwave, active thermography and laser shearography techniques. This is the first time that such prescriptive procedures have been developed and they provide much more information concerning how an inspection should actually be performed and what considerations should be taken into account than existing NDE standards such as ASTM or DIN, particularly for shearography.
- PTB developed completely new capability to enable the simultaneous measurement of spectral emittance and the directional diffuse transmittance for partially transparent materials.
- The thermal conductivity of FRP specimens in all material directions to characterise thermal anisotropy can be measured by CMI using their Small Guarded Hot Plate (SGHP) apparatus.
- Development of new modelling capability by BAM, REG(CEA) and PTB for ultrasonic phased array, microwave and active thermography, enabling theoretical POD assessments to be undertaken.

These outputs will facilitate optimised FRP composites inspection across the energy sectors, thereby increasing confidence in the use of composites and enabling full exploitation and realisation of associated benefits to be achieved. In addition the outputs will support the upskilling of the NDE/composites workforce and stimulate job creation.

Consultancy

Throughout the duration and completion of the project, the consortium has been approached by numerous industry contacts for application advice consultancy and inspection measurement service work for all of the NDE techniques investigated within the VITCEA project. Examples of these interactions include: best practice guidance consultancy for the use of laser shearography for inspection of complex shaped FRP components with a UK based RTO and advice on the application of microwave inspection for marine structures fabricated from GFRP-balsa and GFRP-balsa-metal constructions for a UK based regulator. In addition, meetings have been held between NPL and a Tier 2 member of the UK National Composites Centre (NCC) regarding the potential application of novel techniques included within VITCEA for the inspection of press moulded components.

Industrial Uptake

VITCEA is already having a discernible impact on industry end-users and equipment developers through uptake of the approaches developed within the programme. A presentation on the simulation of microwave inspection based on the work undertaken by Rolf Judaschke at PTB was sent to a supplier of microwave inspection equipment. The work presented highlighted some potential modifications that could be made to the design of microwave transducers to eliminate/reduce unwanted standing wave formations. As a result of these findings, the company have acquired similar modelling software as a tool to improve their equipment design.

Requests have been made by organisations involved with ASTM and ISO standardisation to include aspects of the microwave inspection operational procedure in new or updated standards that either deal solely with microwave inspection or feature microwave inspection as one of the techniques that could be applied to an oil and gas application.

Potential impact

This project has developed operational procedures for NDE techniques which will provide industry with increased confidence in the application of the NDE techniques used for defect detection in a range of FRP composite applications. The project has also increased industry's understanding of how to use NDE techniques, how to interpret their results and what sorts of defects can be detected in a range of different materials.

The project's optimised NDE techniques, operational procedures and modelling capability will lead to improvements in safety, life expectancy, energy efficiency and sustainability; and can contribute to reductions in fossil fuel reliance, greenhouse gas emissions and maintenance costs for FRP assets in the energy sector.

5. Website address and contact details

A public website is available at: http://projects.npl.co.uk/vitcea

The contact person for general questions about the project is Mr Michael Gower (michael.gower@npl.co.uk)

6. List of publications

- Defect characterisation of tensile loaded CFRP and GFRP laminates used in energy applications by means of infrared thermography, Krankenhagen, Maierhofer et al, QIRT Journal, http://dx.doi.org/10.1080/17686733.2017.1334312.
- Hybrid Ray-FDTD Model for the Simulation of the Ultrasonic Inspection of CFRP Parts, Karim JEZZINE, Damien SEGUR, Romain Ecault, Nicolas Dominguez, Proceedings of QNDE16, Atlanta , USA, 17-22nd July 2016, https://doi.org/10.1063/1.4974660.
- Characterisation of artificial defects in CFRP and GFRP sheets designed for energy applications using active thermography, C. Maierhofer, R. Krankenhagen, M. Röllig, B. Rehmer, M. Gower, G. Baker, M. Lodeiro, A. Aktas, L. Knazovická, A. Blahut, C. Monte, A. Adibekyan, B. Gutschwager, Proceedings of Conference QIRT 2016, http://dx.doi.org/10.21611/qirt.2016.076.